

This work has been submitted to the IEEE for possible publication. Copyright may be transferred without notice, after which this version may no longer be accessible.

Submitted to the IEEE Transactions on Automatic Control 8/17/2025.

Observed Control—Linearly Scalable Nonlinear Model Predictive Control with Adaptive Horizons

Eugene T. Hamzezadeh and Andrew J. Petruska

Abstract—This work highlights the duality between state estimation methods and model predictive control. A predictive controller, *observed control*, is presented that uses this duality to efficiently compute control actions with linear time-horizon length scalability. The proposed algorithms provide exceptional computational efficiency, adaptive time horizon lengths, and early optimization termination criteria. The use of Kalman smoothers as the backend optimization framework provides for a straightforward implementation supported by strong theoretical guarantees. Additionally, a formulation is presented that separates linear model predictive control into purely reactive and anticipatory components, enabling *any-time any-horizon observed control* while ensuring controller stability for short time horizons. Finally, numerical case studies confirm that nonlinear filter extensions, i.e., the extended Kalman filter and unscented Kalman filter, effectively extend *observed control* to nonlinear systems and objectives.

Index Terms—Nonlinear Model Predictive Control, Estimation Control Duality, Adaptive Time Horizons, Kalman Filtering, Receding Horizon Control

I. INTRODUCTION

Model predictive control (MPC) is a powerful control strategy that solves finite-horizon optimal control problems online, which enables flexible controllers that can systematically handle constraints, nonlinearities, and multi-input multi-output systems. Historically, MPC emerged from controller developments in the petrochemical and industrial processing industries, where the flexibility, anticipatory behavior, and constraint management are highly valued [1]–[3]. Such systems tend to have longer time constants that afford slower update rates and the direct application of nonlinear optimizers [4]. Often described as “first discretize, then optimize”, this method is known as the *direct method* for MPC [5], [6]. However, interest in applying MPC to faster systems led to the development of online continuation approaches.

Continuation methods for MPC achieve faster update rates by leveraging the similarity of temporally adjacent optimal control problems. With a previous solution’s hot-start, only one Newton-type iteration is performed at each control update

[7], [8]. Real-time iteration (RTI) and related approaches are among the most successful continuation methods [9]–[11]. To achieve increasingly faster update rates, tools to create custom, problem-specific RTI controllers have been presented [12]–[15]. RTI schemes typically scale quadratically with the length of the prediction horizon, as the underlying QP-subproblem grows [16], limiting the use of larger horizon lengths with a notable exception [17]. Additionally, RTI can destabilize if the prediction horizon is too short, if the Newton-type solver converges more slowly than the system dynamics, or if a large disturbance pushes the state outside the contraction region of the underlying Gauss-Newton method [12], [18].

Sampling-based MPC methods make use of Monte Carlo techniques to explore the state and control spaces of systems without requiring explicit gradients, making them compatible with a broad class of systems and objectives. Among these is model predictive path integral (MPPI) control [19] and its variants [20]–[24]. Each update, MPPI algorithms sample a distribution of control sequences, evaluate resulting trajectories, and update the control horizon using the path-integral control framework [25]. A key limitation, however, is the exponential curse of dimensionality in sample size with respect to the prediction horizon length. With inadequate sampling, the control quality suffers, or the controls destabilize entirely. The issue is exacerbated for unstable systems, where high-quality stabilizing samples are rare, making MPPI impractical for systems without significant parallel computing, i.e., a GPU.

Besides the optimization framework, the prediction horizon length N is critical for computational efficiency and closed-loop performance. While terminal costs and constraints can aid in horizon-length stability and optimality proofs [26]–[29], designing terminal constraints for nonstationary references is often intractable, and terminal costs can distort the cost function with respect to the infinite-time original. Stability guarantees with only terminal costs have been established for sufficiently long horizons [30], with subsequent works removing the need for terminal costs altogether [31], [32]. Similarly, sub-optimality bounds have been derived both in the presence [26], [30] and absence [26], [33] of terminal costs, for linear and nonlinear systems. However, all these approaches rely on selecting a fixed N offline, whose sufficiency can only be verified after the optimization, and do not dynamically adapt N to the current state, reference, or system linearization.

To improve MPC’s computational scalability and enable adaptive perfect-length time horizons for closed-loop performance of nonlinear systems, the presented approach leverages duality. Efforts to generalize the classic Kalman-Bucy duality

This work was supported in part by the ARL TBAM-CRP [W911NF-22-2-0235]. (Corresponding author: Eugene T. Hamzezadeh.)

Eugene T. Hamzezadeh and Andrew J. Petruska are with Colorado School of Mines, Golden, CO 80401, USA (e-mails: ehamzeza@mines.edu, apetruska@mines.edu)

[34], [35] include information filters [36], backward stochastic differential equations [37], [38], and variational principles [39]. However, implementable algorithms remain focused on receding horizon schemes. Notably, MPC and moving horizon estimation (MHE) also exhibit a duality; linear MHE over the entire evolution time, termed full information estimation, recovers the Kalman filter [5]. Further, as in MHE, smoothers such as the one developed by Rauch, Tung, and Striebel (RTS) [40] estimate the entire horizon. Crucially, even with nonlinear extensions such as the extended Kalman filter (EKF) [41] and the unscented Kalman filter (UKF) [42], recursive estimators scale linearly with respect to the measurement horizon length. A natural question that follows is: “*What is the control-space dual of recursive smoothers?*” This work proposes *observed control*—a highly efficient predictive control framework that leverages duality with smoothers to produce optimal control actions with linear prediction horizon scalability.

The primary contributions of this work are the four algorithms and related proofs in Section III, which develop the theory behind *observed control* and its implications for MPC in general. The treatment begins with a conceptual forward-backward recursion algorithm in Section III-B, which is simplified to a forward-only approach in Section III-C, and then to a more numerically efficient EKF-specific variant in Section III-F. The forward-only nature of the algorithms enables adaptive prediction horizons based on quantitative metrics that are described in Section III-E. These metrics enable on-the-fly horizon-length adaptation that computes a finite-horizon control to within a desired tolerance of the infinite-horizon optimal, even with nonlinear dynamics, non-quadratic objectives, and nonstationary references. Restricting the analysis to linear time-invariant systems with quadratic costs, Section III-G proves that an optimal linear-quadratic MPC policy is separable into purely reactive and anticipatory components, ensuring closed-loop stability even for minimal one-step horizons. The efficiency and versatility of the presented algorithms are explored in case studies on the predictive control of linear systems (Section IV-A), nonlinear obstacle avoidance objectives (Section IV-B), and nonlinear systems with the canonical cart-pole swing-up problem (Section IV-D). Although an early version of observed control was presented by the authors for magnetic devices [43]; this work provides the first formal presentation of the approach and extends it to support dynamic horizons and any-time any-horizon operation. For readers interested in implementation, the authors recommend starting with Algorithm 2 (Section III-C), as it is compatible with both EKF and UKF computations.

II. PRELIMINARIES

Capital letters A denote matrices; lower case x , vectors. Hats \hat{x} indicate estimates; dots \dot{x} , \ddot{x} time derivatives. Subscripts $x_{k(-)}$, $x_{k(+)}$, $x_{k[s]}$ denote prior, posterior, and smoothed states respectively. The shorthand $\|x\|_A^2$ is $x^\top A x$, and A^\dagger the Moore-Penrose pseudo-inverse $(A^\top A)^{-1} A^\top$. The normal distribution with mean μ and covariance Σ is $\mathcal{N}(\mu, \Sigma)$. All norms are L^2 , written $\|A\|$ without subscripts. Bracketed $u_0^{[N]}$ denotes control u_0 from a prediction horizon of length N . Products $\prod_{i=a}^b$ whose ranges satisfy $b < a$ are the identity \mathbb{I} .

A. Optimal Control

Optimal control is concerned with determining an explicit control law $u = k(x)$ that, for any state x , provides the optimal feedback u to minimize a penalty function $J(x, u)$. Generally, $k(x)$ is found by solving an optimization of the form

$$\arg \min_{u(t)} J(x, u) = \int_{t=0}^{\infty} l(x(t), u(t)) dt \quad (1a)$$

$$\text{subj. to } \dot{x}(t) = f(x(t), u(t)) \quad (1b)$$

$$\{x(t), u(t)\} \in \{\mathcal{X}_k, \mathcal{U}_k\} \quad (1c)$$

where (1a) accumulates the cost function $l(x, u)$, (1b) enforces the dynamics $\dot{x} = f(x, u)$, and (1c) enforces the permissible sets of states \mathcal{X} and controls \mathcal{U} . Unfortunately, an explicit and analytical solution of (1) is rare, but the linear-quadratic case gives the linear quadratic regulator (LQR) solution [44].

B. Model Predictive Control

In contrast to optimal control methods, MPC is an implicit solution technique that approximates (1) with a sequence of smaller finite-horizon problems, and determines the control action $u_i = k_i(x_i)$ by solving a discretized optimization

$$\arg \min_{\{u_0, \dots, u_{N-1}\}} \sum_{k=0}^N J(x_k, u_k) \quad (2a)$$

$$\text{subj. to } x_k = f(x_{k-1}, u_{k-1}) \quad (2b)$$

$$\{x_k, u_k\} \in \{\mathcal{X}_k, \mathcal{U}_k\} \quad (2c)$$

$$x_0 = \hat{x}_0 \quad (2d)$$

at runtime, where N is the length of the finite time horizon and (2d) is an additional initialization constraint with the current state of the system given by \hat{x}_0 . In MPC, feedback is achieved by repeatedly solving (2) as the system evolves [5], [45].

C. State Estimation

State estimators, i.e., observers, determine the instantaneous state \hat{x}_k or sequence of states $\{\hat{x}_0, \dots, \hat{x}_N\}$ that best explain the trajectory of a system given a list of noisy measurements $\{y_0, \dots, y_N\}$. For clarity, the presentation is temporarily restricted to linear systems and measurements; Section III-H provides a nonlinear treatment. Consider the linear system

$$x_k = Ax_{k-1} + Bu_{k-1} + w \quad w \sim \mathcal{N}(0, Q) \quad (3a)$$

$$y_k = Cx_k + v \quad v \sim \mathcal{N}(0, R) \quad (3b)$$

with states $x \in \mathbb{R}^n$, controls $u \in \mathbb{R}^m$, measurements $y \in \mathbb{R}^\nu$, and a discretization period of $\Delta t = t_k - t_{k-1}$. The process noise w and measurement noise v terms are zero-mean, normal distributions with covariances $Q \in \mathbb{R}^{n \times n}$ and $R \in \mathbb{R}^{\nu \times \nu}$.

Moving horizon estimation (MHE) is an optimization-based estimator concerned with producing only the last N state estimates $\hat{X} = \{\hat{x}_{T-N}, \hat{x}_{T-N+1}, \dots, \hat{x}_T\}$ considering only the last N measurements $Z = \{y_{T-N}, y_{T-N+1}, \dots, y_T\}$. The problem is often given as an optimization of the form

$$\arg \min_{\{\hat{x}_{T-N}, \dots, \hat{x}_T\}} J = \sum_{k=T-N}^N l(y_k - C\hat{x}_k) \quad (4a)$$

$$\text{subj. to } x_k = Ax_{k-1} + Bu_{k-1} \quad (4b)$$

where $l(r)$ is often a quadratic loss function of the residuals $r_k = y_k - Cx_k$. When $N = T$, the problem is termed full information estimation. However, the problem scales poorly with N , so recursive estimators such as the well-known Kalman filter are preferred for real-time applications.

Recursive estimators find the next state estimate \hat{x}_{k+1} as a function of only the current state estimate \hat{x}_k and incoming measurement y_{k+1} . To enable this, they also track estimate uncertainty, i.e., covariance P_k , over time. Additionally, most implementations separate the filter into prediction (prior) and measurement (posterior) steps, providing estimates when measurements are not yet available. The following algorithmic development centers around the Kalman filter; a brief review of the well-known equations is therefore provided [34], [35]. The mean and covariance prediction equations are given by

$$x_{k(-)} = Ax_{k-1(+)} + Bu_{k-1} \quad (5a)$$

$$P_{k(-)} = AP_{k-1(+)}A^\top + Q \quad (5b)$$

When a new measurement y_k arrives, the anticipated measurement residual r_k is given by

$$r_k = y_k - C\hat{x}_{k(-)} \quad (5c)$$

The posterior prediction and covariance are produced with

$$x_{k(+)} = x_{k(-)} + K_k r_k \quad (5d)$$

$$P_{k(+)} = (\mathbb{I} - K_k C)P_{k(-)} \quad (5e)$$

where K_k is the Kalman gain

$$K_k = P_{k(-)}C^\top(CP_{k(-)}C^\top + R)^{-1} \quad (5f)$$

However, like in MHE, the estimate for \hat{x}_k can be improved by incorporating future measurements $\{y_{k+1}, \dots, y_N\}$. Perhaps the most commonly used Kalman smoother is the one developed by Rauch, Tung, and Striebel (RTS) [40]. Whereas previous smoothers ran two filters—combining the results of a forward-in-time and backward-in-time pass—the RTS smoother is formulated to only use information from the forward filter pass. Also expressed as a recursion, operating backwards in time, the relevant smoother equations are

$$L_k = P_{k(+)}A_k^\top P_{k+1(-)}^{-1} \quad (6a)$$

$$\hat{x}_{k[s]} = \hat{x}_{k(+)} + L_k(\hat{x}_{k+1[s]} - \hat{x}_{k+1(-)}) \quad (6b)$$

$$P_{k[s]} = P_{k(+)} + L_k(P_{k+1[s]} - P_{k+1(-)})L_k^\top \quad (6c)$$

where L_k is the RTS smoother gain. The RTS smoother is initialized by setting the last smoothed estimate $\hat{x}_{N[s]}$ to the last posterior $\hat{x}_{N(+)}$. Then, to produce the set of smoothed state estimates $\{x_{0[s]}, \dots, x_{N[s]}\}$, equations (6b-6a) are iterated backwards to $k = 0$. Kalman smoothers of this type are known to minimize the loss function

$$J(x_0, \dots, x_N) = \|(x_0 - \hat{x}_0)\|_{P_0^{-1}}^2 \quad (7a)$$

$$+ \sum_{k=0}^N \|z_k - C\hat{x}_k\|_{R^{-1}}^2 \quad (7b)$$

$$+ \sum_{k=0}^{N-1} \|x_{k+1} - A\hat{x}_k\|_{Q^{-1}}^2 \quad (7c)$$

where the terms (7a) and (7c) penalize the estimation errors and (7b) penalizes the measurement residuals [46].

III. OBSERVED CONTROL

The key idea behind observed control is to cast predictive control problems as state estimation tasks. The framework uses a forward filter pass to estimate future states, *measures* expected cost functions of those states, and uses a smoother pass to *estimate* the control sequence which minimizes the estimation error. That is, from the maximum likelihood perspective, to find the controls that are most likely to result in the measurements, i.e., the objective function. To enable this, the dynamics constraints (2b) will be encoded into (7a) and (7c) while the objective function (2a) will be encoded into the residuals (7b). This construction effectively makes observed control's objective function (7) and the mapping of the MPC formulation (2) into this estimation-based form is central to using smoothers to solve predictive control problems.

The following development maps linear-quadratic control problems—such as the standard LQR formulation—into equivalent smoother formulations. This canonical example introduces the augmentation concepts of the observed control framework and sets the stage for the rest of the paper. At this point, the analysis remains restricted to linear time-invariant systems of the form

$$x_k = Ax_{k-1} + Bu_{k-1} \quad (8a)$$

$$y_k = Cx_k + Du_k \quad (8b)$$

with n states, m controls, and ν measurements. To use the observed control framework to *estimate controls*, the number of augmented states is defined as $\eta = n + m$ and the number of augmented measurements as $\mu = \nu + m$. The augmented system state χ_k and system matrices Φ and H are defined as

$$\chi_k = \begin{bmatrix} x_k \\ u_k \end{bmatrix} \quad \Phi = \begin{bmatrix} A & B \\ 0 & \mathbb{I}_m \end{bmatrix} \quad H = \begin{bmatrix} C & D \\ 0 & \mathbb{I}_m \end{bmatrix} \quad (9)$$

where $\chi \in \mathbb{R}^\eta$, $\Phi \in \mathbb{R}^{\eta \times \eta}$, and $H \in \mathbb{R}^{\mu \times \eta}$. The augmented model used for filtering and smoothing is given by

$$\chi_k = \Phi\chi_{k-1} + \dot{w} \quad \dot{w} \sim \mathcal{N}(0, \dot{Q}) \quad (10a)$$

$$z_k = H\chi_k + \dot{v} \quad \dot{v} \sim \mathcal{N}(0, \dot{R}) \quad (10b)$$

where \dot{w} and \dot{v} are the zero-mean plant and measurement noise terms with covariances $\dot{Q} \in \mathbb{R}^{\eta \times \eta}$ and $\dot{R} \in \mathbb{R}^{\mu \times \mu}$ respectively.

A. Reduction to LQR

Given observed control's use of Kalman smoothers for the optimization of controls and the well-known duality between the Kalman filter and linear quadratic regulator, it only seems natural to explain the mapping of cost functions and constraints within the observed control framework using LQR as an example. This will inform the construction of the underlying Kalman filter covariance matrices (P_0 , Q , and R), while demonstrating how observed control optimally solves linear-quadratic control problems. Consider the discrete-time reference tracking LQR formulation given by

$$\arg \min_{u_0} \sum_{k=0}^{\infty} \left(\|x_r - x_k\|_{Q_{[\text{lqr}]}}^2 + \|u_k\|_{R_{[\text{lqr}]}}^2 + 2x_k^T M_{[\text{lqr}]} u_k + \|u_k - u_{k-1}\|_{\tilde{R}_{[\text{lqr}]}}^2 \right) \quad (11a)$$

$$\text{subj. to } x_k = Ax_{k-1} + Bu_{k-1} \quad (11b)$$

where x_r is the desired reference and $Q_{[lqr]}$, $R_{[lqr]}$, and $M_{[lqr]}$, $\tilde{R}_{[lqr]}$ are the penalty weighting matrices on state, control, state-control coupling, and control rate respectively.

Theorem 1. *With a constant reference, observed control's smoother objective (7) converges to the general discrete LQR problem (11) as the horizon length $N \rightarrow \infty$ when $P_0 = \dot{Q}$ and the filter covariance matrices \dot{Q} and \dot{R} are selected as*

$$\dot{R} = \begin{bmatrix} Q_{[lqr]} & M_{[lqr]} \\ M_{[lqr]}^\top & R_{[lqr]} \end{bmatrix}^{-1} \quad \dot{Q} = \begin{bmatrix} \mathbb{O}_n & 0 \\ 0 & \tilde{R}_{[lqr]}^{-1} \end{bmatrix} \quad (12)$$

Proof. Examining the augmented form of the smoother loss (7), and the LQR formulation (11), the apparent discrepancies are the number of terms in the LQR objective (11a) and the addition of the constraint (11b). Assuming identical initial and step process noises, $P_0 = \dot{Q}$, and the summations (7a) and (7c) combine. Since LQR traditionally assumes full-state feedback and penalizes every state and control, the full-state measurement z_k and its sensitivity H_k are given by

$$z_k = \begin{bmatrix} x_r^\top & \bar{0}_m^\top \end{bmatrix}^\top \quad H_k = \mathbb{I}_\eta \quad (13)$$

and the smoother loss function (7) can be re-written as

$$J(\chi_0, \dots, \chi_N) = \sum_{k=0}^N \|z_k - \hat{\chi}_k\|_{\tilde{R}^{-1}}^2 \quad (14a)$$

$$+ \sum_{k=0}^N \|\chi_k - \hat{\chi}_k\|_{\dot{Q}^{-1}}^2 \quad (14b)$$

noting the summation's range change (14b) and the use of the augmented system (9). The augmented residual r_k is given by

$$r_k = z_k - H_k \hat{\chi}_k \quad (15)$$

The first three terms of the LQR penalty function (11a) are encoded in (14a) by selecting

$$\dot{R}^{-1} = \begin{bmatrix} Q_{[lqr]} & M_{[lqr]} \\ M_{[lqr]}^\top & R_{[lqr]} \end{bmatrix} \quad (16)$$

while the LQR dynamics constraint (11b) and control rate penalty term are encoded into (14b) by selecting

$$\dot{Q}^{-1} = \begin{bmatrix} \beta \mathbb{I}_{n \times n} & 0 \\ 0 & \tilde{R}_{[lqr]} \end{bmatrix} \quad (17)$$

and letting $\beta \rightarrow \infty$. In this limit, the dynamics-prediction errors are infinitely penalized, enforcing the constraint (11b), and the inverse becomes identically \mathbb{O}_n . Therefore, (12) provides the \dot{R} and \dot{Q} to be used in observed control that optimally solves the linear-quadratic control problem given the firmly established optimality of LQR and RTS [40], [47]. \square

Remark. *If there are states and controls that should not be penalized, then a full-sized \dot{R}^{-1} is rank deficient. However, the information that states and controls should be excluded from the optimization can be shifted from the weighting matrix \dot{R}^{-1} to the measurement sensitivity H_k so as not to measure them. Thus, \dot{R}^{-1} should be reduced to only penalize the states and controls of interest, and H_k and z_k should be appropriately selected to ignore unpenalized combinations.*

Algorithm 1 Naïve Observed Control

```

initialize  $\chi_{0(-)} \leftarrow [\hat{x}^\top \quad u_{\text{last}}^\top]^\top$ ,  $P_{0(-)} \leftarrow \dot{Q}$ 

for  $k \in [0, \dots, N]$  do ▷ Kalman filter pass
  if  $k > 0$  then
     $\chi_{k(-)} \leftarrow \Phi_{k-1} \chi_{k-1(+)}$  ▷ (5a)
     $P_{k(-)} \leftarrow \Phi_{k-1} P_{k-1(+)} \Phi_{k-1}^\top + \dot{Q}$  ▷ (5b)
     $K_k = P_{k(-)} H_k^\top [H_k P_{k(-)} H_k^\top + \dot{R}]^{-1}$  ▷ (5f)
     $r_k \leftarrow z_k - H_k \chi_{k-1(-)}$  ▷ (5c)
     $\chi_{k(+)} \leftarrow \chi_{k(-)} + K_k r_k$  ▷ (5d)
     $P_{k(+)} \leftarrow [\mathbb{I} - K_k H_k] P_{k(-)}$  ▷ (5e)
  for  $k \in [N-1, \dots, 0]$  do ▷ RTS smoother pass
     $L_k = P_{k(+)} \Phi_k^\top P_{k+1(-)}^{-1}$  ▷ (6a)
     $\chi_{k[s]} \leftarrow \chi_{k(+)} + L_k (\chi_{k[s]+1} - \chi_{k+1(-)})$  ▷ (6b)
     $P_{k[s]} \leftarrow P_{k(+)} + L_k (P_{k[s]+1} - P_{k+1(-)}) L_k^\top$  ▷ (6c)
return  $u_0 \in \chi_{0[s]}$ 

```

Remark. *The weighting matrix $\tilde{R}_{[lqr]}$ penalizes Δu and cannot be eliminated completely for numerical stability. In practice, a Δu penalty is desirable to avoid control chatter while choosing $\tilde{R}_{[lqr]}$ to be multiple orders of magnitude smaller than any term in \dot{R} renders it effectively negligible.*

B. Smoother Derived Naïve Observed Control

Algorithm 1—*naïve observed control*—implements an RTS smoother directly on the augmented system (10) with measurement and process noise defined by (12). The algorithm initializes a Kalman filter with the current state and previously applied control and performs a forward filter pass, equations (5a)-(5f), taking measurements as the desired state z_k over a time horizon of length N as in (15). It then initializes an RTS smoother with the final-time smoothed estimate given by $\chi_{N[s]} = \chi_{N(+)}$ and performs the smoother equations (6b)-(6a) back to time $k = 0$. The desired control action is contained in the smoothed state $\chi_{0[s]}$ and can be applied to the system.

C. Forward Only General Observed Control

While Algorithm 1 is sufficient to compute the optimal predictive control update, it leaves room for computational and numerical stability improvements. In the MPC scheme, only the first control in the optimization horizon is ever applied to the system before the next optimization cycle. That is, refinements to the controls in the intermediate smoothed results $\{\chi_{1[s]} \dots \chi_{N[s]}\}$ need not be explicitly computed. Re-examining the RTS smoother state update equations with this insight, the initial control $\chi_{0[s]}$ can be extracted by recursively substituting equation (6b) with future versions of itself, yielding the relationship

$$\begin{aligned}
 \chi_{0[s]} &= \chi_{0(+)} + L_0 (\chi_{1[s]} - \chi_{1(-)}) \\
 &= \chi_{0(+)} + L_0 ([\chi_{1(+)} + L_1 (\chi_{2[s]} - \chi_{2(-)})] - \chi_{1(-)}) \\
 &= \chi_{0(+)} + L_0 (\chi_{1(+)} - \chi_{1(-)}) \\
 &\quad + L_0 L_1 (\chi_{2(+)} - \chi_{2(-)}) \\
 &\quad + L_0 L_1 L_2 (\chi_{3(+)} - \chi_{3(-)}) + \{\dots\}
 \end{aligned} \quad (18)$$

which highlights the individual contributions of each future measurement in the receding horizon ($k \geq 1$) to the present-time smoothed state ($k = 0$). In general, for N measurements, the smoothed augmented state can be described by

$$\chi_{0[s]} = \chi_{0(+)} + \sum_{k=1}^N \left(\prod_{i=0}^{k-1} L_i \right) (\chi_{k(+)} - \chi_{k(-)}) \quad (19a)$$

$$u_{0[s]} = u_{0(+)} + \sum_{k=1}^N \Gamma_{k-1} (\chi_{k(+)} - \chi_{k(-)}) \quad (19b)$$

where the accumulator Γ_k can be recursively found with

$$\Gamma_k = \Gamma_{k-1} L_k \quad \Gamma_{-1} \equiv [\mathbb{O} \quad \mathbb{I}]_{m \times n} \quad (20)$$

The matrix Γ_{-1} can be initialized in this manner because the initial process noise P_0 has no uncertainty in the states $x_0 \in \chi_0$, see (12) in Theorem 1. Thus, the product $\prod_{i=0}^{k-1} L_i$ is identically zero for the top n rows corresponding to updates in the initial states x_0 , which need not be explicitly carried out during the computation.

The relationship (19b) removes the need for a separate smoother pass as the gain product Γ_k can be accumulated with information only from the forward pass. A similar relationship for the smoothed initial controls covariance $P_{uu0[s]}$ can be found by recursively substituting (6c), yielding a forward-only update on both the initial state (control) and state-uncertainty at each step k in the receding horizon

$$u_{0[s]} \leftarrow u_{0[s]} + \Gamma_{k-1} (\chi_{k(+)} - \chi_{k(-)}) \quad (21)$$

$$P_{uu0[s]} \leftarrow P_{uu0[s]} + \Gamma_{k-1} (P_{k(+)} - P_{k(-)}) \Gamma_{k-1}^\top \quad (22)$$

Using these recursive relationships, Algorithm 2—*forward-only observed control*—is developed, which is preferred to the naïve algorithm as it only requires a single forward-in-time filter pass, does not spend time refining future controls $\{u_1, \dots, u_{N-1}\}$ that will be discarded, and only smooths controls, not states.

The accumulator Γ_k defines how future measurements (cost function evaluations) map to the current control action and informs the rate of convergence in the initial state uncertainty, or covariance. Understanding how this gain converges is the topic of Section III-D and informs adaptive time horizons and early termination metrics discussed in Section III-E, but are included in Algorithm 2 for implementation completeness.

D. Convergence of Forward Pass

The control action $u_{0[s]}$ and uncertainty $P_{uu0[s]}$ are dependent on the convergence of the series in (21) and (22) which are ultimately dominated by the smoother gain product Γ_k in (20). As $k \rightarrow \infty$, it can be shown that $\Gamma_k \rightarrow 0$, which yields useful properties for informing appropriate horizon lengths.

Lemma 1. *The sequence of smoother gains $\{L_0, L_1, \dots, L_N\}$ converges to an infinite time value of L_∞ given by*

$$L_\infty = P_{\infty(+)} \Phi^\top P_{\infty(+)}^{-1} (\mathbb{I} - K_\infty H) \quad (23)$$

which depends solely on the system matrices (Φ, H) , and the convergence of the Kalman gain to K_∞ .

Algorithm 2 Forward-Only Observed Control

initialize $\chi_{0(-)} \leftarrow [\hat{x}^\top \quad u_{\text{last}}^\top]^\top$, $u_{0[s]} \leftarrow u_{\text{last}}$,
 $P_{0(-)} \leftarrow \hat{Q}$, $P_{0[s]} \leftarrow \hat{Q}$, $\Gamma_{-1} \leftarrow [\mathbb{O} \quad \mathbb{I}]$

for $k \in [0, \dots, N]$ **do** ▷ Single Forward Pass
if $k > 0$ **then**
 $\chi_{k(-)} \leftarrow \Phi_{k-1} \chi_{k-1(+)} \quad \triangleright (5a)$
 $P_{k(-)} \leftarrow \Phi_{k-1} P_{k-1(+)} \Phi_{k-1}^\top + \hat{Q} \quad \triangleright (5b)$
 $\Gamma_{k-1} \leftarrow \Gamma_{k-2} (P_{k-1(+)} \Phi_{k-1}^\top P_{k(-)}^{-1}) \quad \triangleright (20)$
 $r_k \leftarrow z_k - H_k \chi_{k(-)} \quad \triangleright (5c)$
 $K_k \leftarrow P_{k(-)} H_k^\top [H_k P_{k(-)} H_k^\top + \hat{R}_k]^{-1} \quad \triangleright (5f)$
 $\chi_{k(+)} \leftarrow \chi_{k(-)} + K_k r_k \quad \triangleright (5d)$
 $P_{k(+)} \leftarrow [\mathbb{I} - K_k H_k] P_{k(-)} \quad \triangleright (5e)$
 $u_{0[s]} \leftarrow u_{0[s]} + \Gamma_{k-1} (\chi_{k(+)} - \chi_{k(-)}) \quad \triangleright (21)$
 $P_{uu0[s]} \leftarrow P_{uu0[s]} + \Gamma_{k-1} (P_{k(+)} - P_{k(-)}) \Gamma_{k-1}^\top \quad \triangleright (22)$
 $\rho_k \leftarrow \|\Gamma_{k-1} K_k\| \quad \triangleright (45)$
 $\tau_k \leftarrow \text{tr}(\Gamma_{k-1} (P_{k(-)} - P_{k(+)})) / \text{tr}(P_{0[s]}) \quad \triangleright (47)$
if $\rho_k \leq \delta_1$ **and** $\tau_k \leq \delta_2$ **break** ▷ Early Termination

return $u_{0[s]}$

Proof. The infinite-time Kalman gain K_∞ converges if $Q \succeq 0$, $R \succ 0$, the pair (Φ, H) is detectable, and the pair $(A, Q^{1/2})$ is stabilizable. The convergence of K_∞ establishes the convergence of both $P_{\infty(-)}$ and $P_{\infty(+)}$ to finite values satisfying the posterior update equation (5e). Rearranging the infinite-time version of (5e) yields

$$P_{\infty(-)}^{-1} = P_{\infty(+)}^{-1} (\mathbb{I} - K_\infty H) \quad (24)$$

which can be substituted into the infinite-time version of (6a)

$$L_\infty = P_{\infty(+)} \Phi^\top P_{\infty(-)}^{-1} \quad (25)$$

yielding the desired result

$$L_\infty = P_{\infty(+)} \Phi^\top P_{\infty(+)}^{-1} (\mathbb{I} - K_\infty H) \quad (26)$$

which completes the proof. \square

Lemma 2. *Given the convergence of the Kalman filter and a detectable (Φ, H) , the matrix expressions*

$$L_\infty = P_{\infty(+)} \Phi^\top P_{\infty(+)}^{-1} (\mathbb{I} - K_\infty H) \quad (27)$$

$$A^* = \Phi^\top (\mathbb{I} - H^\top K_\infty^\top) \quad (28)$$

for the infinite-time smoother gain L_∞ and the given closed loop system, respectively, have the same eigenvalues.

Proof. Two matrices L_∞ and A^* have the same eigenvalues if there exists a V such that $L_\infty = V A^* V^{-1}$. Choosing $V = P_{\infty(+)}$, the product $V A^* V^{-1}$ becomes

$$V A^* V^{-1} = P_{\infty(+)} (\Phi^\top - \Phi^\top H^\top K_\infty^\top) P_{\infty(+)}^{-1} \quad (29)$$

Comparing with the expanded (27) given by

$$L_\infty = P_{\infty(+)} \Phi^\top P_{\infty(+)}^{-1} - P_{\infty(+)} \Phi^\top P_{\infty(+)}^{-1} K_\infty H \quad (30)$$

and explicitly setting $L_\infty = VA^*V^{-1}$ yields the equality

$$P_{\infty(+)}^{-1}K_\infty H = H^\top K_\infty^\top P_{\infty(+)}^{-1} \quad (31)$$

with cancellations omitted. Rearranging yields

$$K_\infty H = P_{\infty(+)} H^\top K_\infty^\top P_{\infty(+)}^{-1} \quad (32)$$

Substituting $P_{\infty(+)} = (\mathbb{I} - K_\infty H)P_{\infty(-)}$, the infinite time prior-posterior relationship given by (5e), yields

$$K_\infty H = [(\mathbb{I} - K_\infty H)P_{\infty(-)}] K_\infty^\top [(\mathbb{I} - K_\infty H)P_{\infty(-)}]^{-1} \quad (33)$$

which, with rearranging, results in

$$K_\infty H = P_{\infty(-)} H^\top K_\infty^\top P_{\infty(-)}^{-1} \quad (34)$$

Substituting the infinite time Kalman gain equation (5f) on the right $K_\infty = P_{\infty(-)} H^\top (HP_{\infty(-)} H^\top + \dot{R})^{-1}$ yields

$$\begin{aligned} K_\infty H &= P_{\infty(-)} \left[P_{\infty(-)} H^\top (HP_{\infty(-)} H^\top + \dot{R})^{-1} \right]^\top P_{\infty(-)}^{-1} \\ &= P_{\infty(-)} (HP_{\infty(-)} H^\top + \dot{R})^{-T} HP_{\infty(-)}^\top P_{\infty(-)}^{-1} \quad (35) \\ &= P_{\infty(-)} (HP_{\infty(-)} H^\top + \dot{R})^{-1} H \\ &= K_\infty H \end{aligned}$$

which completes the proof. \square

Theorem 2. *If the infinite time stabilizing Kalman gain K_∞ exists, there exists an infinite time smoother gain L_∞ with all stable eigenvalues, that is $|\lambda_i| < 1$ for all $i \in [0, \eta - 1]$.*

Proof. Consider the open-loop system given by

$$x_{k+1}^* = \Phi^\top x_k^* + \Phi^\top H^\top u^* \quad (36)$$

which is stabilized using the LQR objective function

$$J(x^*, u^*) = x^{*T} Q^* x^* + u^{*T} R^* u^* + 2x^{*T} S^* u^* \quad (37)$$

where weights $Q^* = \dot{Q}$, $R^* = H\dot{Q}H^\top + \dot{R}$, and $S^* = \dot{Q}H^\top$. Stabilizing closed loop poles are guaranteed to exist as if the pair $(\Phi^\top, \Phi^\top H^\top)$ is stabilizable, the and the expressions $H\dot{Q}H^\top + \dot{R}$ and $\dot{Q} - \dot{Q}H^\top (H\dot{Q}H^\top + \dot{R})^{-1} H\dot{Q}$ are positive definite. If additionally, there are no unobservable nodes on the unit circle, then the stabilizing LQR feedback gain K_f exists and is given by

$$K_f = (H\Phi P_{\infty(+)} \Phi^\top H^\top + H^\top \dot{Q} H^\top + R)^{-1} (H\Phi P_{\infty(+)} \Phi^\top + H\dot{Q}) \quad (38)$$

and the stable closed-loop system is given by

$$\Phi^\top (\mathbb{I} - H^\top K_f) \quad (39)$$

Observing that K_f , given by (38), is the transpose of the Kalman gain in (5f) for the system given by (36), and applying Lemma 2, it follows that the eigenvalues of the infinite-time smoother gain L_∞ are equivalent to those of the closed-loop system (39). Therefore, the eigenvalues of L_∞ are also guaranteed to be stable and lie within the unit circle. \square

Corollary 2.1. *For a given controllable, stabilizable, and observable system and an arbitrarily small $\delta_1 > 0$, there exists*

a time horizon of length N such that the difference in controls given the time horizon lengths N and $N - 1$ satisfies

$$\|u_0^{[N]} - u_0^{[N-1]}\| \leq \delta_1 \quad (40)$$

to the desired convergence tolerance of δ_1 .

Proof. By Theorem 2, the eigenvalues $\{\lambda_0, \dots, \lambda_{\eta-1}\}$ of the smoother gain L_N are guaranteed to satisfy $\|\lambda_i\| < 1$ for all $i \in [0, \eta - 1]$ as $N \rightarrow \infty$. Therefore, it follows that the gain term can be partitioned by an index b into two groups:

$$\Gamma_k = [\mathbb{O} \quad \mathbb{I}]_{m \times \eta} \left(\prod_{i=0}^{b-1} L_i \right) \left(\prod_{i=b}^k L_i \right) \quad (41)$$

where all the terms $i \geq b$ will contain sufficiently-converged stable eigenvalues satisfying $|\lambda_i| < 1$ and thus will force the convergence of $\Gamma_{N-1} \rightarrow \mathbb{O}$ as $N \rightarrow \infty$. Since $\Gamma_{N-1} \rightarrow \mathbb{O}$, it follows that the $\Gamma_{k-1}(\chi_{k(+)} - \chi_{k(-)})$ terms of the summation in the forward pass update equation (21) will also tend to $\vec{0}$ as $N \rightarrow \infty$. Therefore, the difference in applied control between adjacent horizon lengths $\|u_0^{[N]} - u_0^{[N-1]}\|$ vanishes. \square

Corollary 2.2. *The difference in the initial-time smoother covariance $P_{0[s]}$ given two adjacent time horizon lengths of N and $N - 1$ will converge to \mathbb{O} as the length of the time horizon $N \rightarrow \infty$. That is, the expression*

$$\Psi_N = P_{0[s]}^{[N]} - P_{0[s]}^{[N-1]} \quad (42)$$

converges to \mathbb{O} geometrically as $N \rightarrow \infty$ independent of system stability or controllability.

Proof. In a similar argument to that of Corollary 2.1, the convergence of the gain term $\Gamma_{N-1} \rightarrow 0$ as $N \rightarrow \infty$ ensures that the individual terms $\Gamma_{k-1}(P_{k(-)} - P_{k(+)})\Gamma_{k-1}^\top$ in the summation of the smoother covariance equation (22) will geometrically converge to \mathbb{O} . It then follows that the initial-time smoother covariance will converge to an infinite-horizon value of $P_{0[s]}^{[\infty]}$. Therefore, $P_{0[s]}^{[N]} - P_{0[s]}^{[N-1]}$, the difference between adjacent horizon-length initial-time smoothed covariances, will tend to \mathbb{O} as $N \rightarrow \infty$. If the system pair (A, B) is uncontrollable, the augmented pair $(\Phi, \Phi H)$ becomes undetectable and $P_{0[s]}$ will not converge in the undetectable states as $N \rightarrow \infty$, due to the presence of eigenvalues on the unit circle. However, the difference Ψ will still always converge to \mathbb{O} . \square

E. Early Termination Criteria

The posterior-prior difference $\chi_{k(+)} - \chi_{k(-)}$ can be written in terms of the Kalman gain, yielding the relation

$$\chi_{k(+)} - \chi_{k(-)} = K_k r_k \quad (43)$$

where the residual r_k as in (15) is the anticipated reference tracking error shown in Theorem 1. Expressing the recursive forward-only control refinement (21) using (43) yields

$$u_{0[s]} \leftarrow u_{0[s]} + \Gamma_{k-1} K_k r_k \quad (44)$$

which highlights how future measurement residuals r_k no longer impact the control u_0 when $\|\Gamma_{k-1} K_k\| \approx 0$. Corollary

2.1 proves that $\|\Gamma_k\| \rightarrow 0$ as $k \rightarrow \infty$, justifying the choice of a δ_1 threshold for the early termination metric ρ given by

$$\rho_N = \|\Gamma_{N-1} K_N\| \quad (45)$$

that determines a sufficient predictive look ahead N . In practice, the threshold δ_1 should be chosen based on desired control smoothness, i.e. the maximum Δu_0 permissible given an unanticipated change in reference at time $N + 1$.

The convergence of $P_{0[s]}^{[N]}$ as $N \rightarrow \infty$ parallels the convergence of LQR's cost-to-go Riccati equation, making Ψ a valuable metric for determining when u_0 has reached an effective infinite-time equivalence. Corollary 2.2 defines a first-order optimality condition on $P_{0[s]}$ informing the convergence threshold δ_2 based on the normalized value τ given by

$$\tau_k = \text{tr}(\Psi) / \text{tr}(P_{0[s]}^{[k]}) \quad (46)$$

$$\tau_k = \text{tr}(\Gamma_{k-1}(P_{k(+)} - P_{k(-)})\Gamma_{k-1}^\top) / \text{tr}(P_{0[s]}^{[k]}) \quad (47)$$

where $\tau_k \approx 0$ ensures that the algorithm has sufficiently approximated infinite-time regulating control.

F. Efficient EKF-Based Observed Control

While Algorithms 1 and 2 provide for a straightforward implementation, further efficiency and numerical stability can be gained by analyzing the structure of the smoother gain accumulator Γ_k . As given in (20), the accumulator is intuitively the product of the individual RTS smoother gains $\{L_0, \dots, L_k\}$; however, the inverse priors in each L_i , $i \in [0, k]$ are expensive to evaluate and accumulate numerical sensitivity. Expanding the first few terms of the smoother gain accumulator (20) gives

$$\Gamma_k = \Gamma_{-1} P_{0(+)} \Phi_0^\top P_{1(-)}^{-1} P_{1(+)} \Phi_1^\top P_{2(-)}^{-1} \prod_{i=2}^k L_i. \quad (48)$$

Replacing each $P_{k(+)}$ with the transpose of (5e) yields

$$\begin{aligned} \Gamma_k &= \Gamma_{-1} P_{0(-)} (\mathbb{I} - K_0 H_0)^\top \Phi_0^\top P_{1(-)}^{-1} \\ &\quad P_{1(-)}^\top (\mathbb{I} - K_1 H_1)^\top \Phi_1^\top P_{2(-)}^{-1} \prod_{i=2}^k L_i \end{aligned} \quad (49)$$

$$\begin{aligned} &= \Gamma_{-1} P_{0(-)} (\mathbb{I} - K_0 H_0)^\top \\ &\quad \left(\prod_{i=1}^k \Phi_{i-1}^\top (\mathbb{I} - K_i H_i)^\top \right) \Phi_k^\top P_{k+1(-)}^{-1} \end{aligned} \quad (50)$$

Defining $\Phi_{-1} \equiv \mathbb{I}$, the smoother gain accumulator becomes

$$\Gamma_k = \Gamma_{-1} P_{0(-)} \left(\prod_{i=0}^k \Phi_{i-1}^\top (\mathbb{I} - K_i H_i)^\top \right) \Phi_k^\top P_{k+1(-)}^{-1} \quad (51)$$

Expanding the Kalman gain in (43) with (5f) yields

$$\chi_{k(+)} - \chi_{k(-)} = P_{k(-)} H_k^\top (H_k P_{k(-)} H_k^\top + \dot{R})^{-1} r_k \quad (52)$$

Combining (52) with the improved gain accumulator (51) and substituting into equation (21) gives the result

$$u_{0[s]} = u_{0(+)} + \sum_{k=1}^N [G_{k-1} \Phi_{k-1}^\top S_k r_k] \quad (53)$$

Algorithm 3 Efficient Observed Control

initialize $\chi_{0(-)} \leftarrow [\hat{x} \quad u_{\text{last}}]^\top$, $P_{0(-)} \leftarrow \dot{Q}$,
 $\text{tr}(P_{0[s]}) \leftarrow \text{tr}(P_{0(-)})$, $u_{0[s]} \leftarrow u_{\text{last}}$, $G_{-1} \leftarrow [\mathbb{O} \quad \mathbb{I}] \dot{Q}$

for $k \in [0, \dots, N]$ **do** ▷ Single Forward Pass
if $k > 0$ **then**
 $\chi_{k(-)} \leftarrow \Phi_{k-1} \chi_{k-1(+)} \quad \triangleright (5a)$
 $P_{k(-)} \leftarrow \Phi_{k-1} P_{k-1(+)} \Phi_{k-1}^\top + \dot{Q} \quad \triangleright (5b)$
 $r_k \leftarrow z_k - H_k \chi_{k-1(-)} \quad \triangleright (5c)$
 $S_k \leftarrow H_k^\top [H_k P_{k(-)} H_k^\top + \dot{R}]^{-1} \triangleright \text{Only Inverse } (54e)$
 $K_k \leftarrow P_{k(-)} S_k \quad \triangleright (55)$
 $\chi_{k(+)} \leftarrow \chi_{k(-)} + K_k r_k \quad \triangleright (5d)$
 $P_{k(+)} \leftarrow [\mathbb{I} - K_k H_k] P_{k(-)} \quad \triangleright (5e)$
 $\Psi_k \leftarrow G_{k-1} \Phi_{k-1}^\top S_k H_k \Phi_{k-1} G_{k-1}^\top \quad \triangleright \Delta P_{0[s]}$
 $u_{0[s]} \leftarrow u_{0[s]} + G_{k-1} \Phi_{k-1}^\top S_k r_k \quad \triangleright (53)$
 $\text{tr}(P_{0[s]}) \leftarrow \text{tr}(P_{0[s]}) - \text{tr}(\Psi_k) \quad \triangleright (58)$
 $\rho_k \leftarrow \|G_{k-1} \Phi_{k-1}^\top S_k\| \quad \triangleright (59)$
 $\tau_k \leftarrow \text{tr}(G_{k-1} \Phi_{k-1}^\top S_k H_k \Phi_{k-1} G_{k-1}^\top) / \text{tr}(P_{0[s]}) \triangleright (60)$
if $\rho \leq \delta_1$ **and** $\tau_k \leq \delta_2$ **break** ▷ Early Termination
 $G_k = G_{k-1} \Phi_{k-1}^\top (\mathbb{I} - K_k H_k)^\top \quad \triangleright (54d)$

return $u_{0[s]}$

where G_k and S_k are the inverse free gain and the observed innovation matrices, respectively, given by

$$\Phi_{-1} \equiv \mathbb{I} \quad (54a)$$

$$G_{-1} \equiv [\mathbb{O} \quad \mathbb{I}] P_{0(-)} \quad (54b)$$

$$G_k = [\mathbb{O} \quad \mathbb{I}] P_{0(-)} \prod_{i=0}^k \Phi_{i-1}^\top (\mathbb{I} - K_i H_i)^\top \quad (54c)$$

$$G_k = G_{k-1} \Phi_{k-1}^\top (\mathbb{I} - K_k H_k)^\top \quad (54d)$$

$$S_k = H_k^\top (H_k P_{k(-)} H_k^\top + \dot{R})^{-1} \quad (54e)$$

Although this reformulation appears messier, it requires only one inverse per time horizon update in S_k , which is guaranteed to be well-defined by the positive-definite \dot{R} . This single inverse can be reused in the Kalman gain calculation, giving

$$K_k = P_{k(-)} S_k \quad (55)$$

As in (21), all required information can be accumulated from the forward filter pass, minimizing computational burden.

A similar result for the forward-in-time update of the smoothed covariance $P_{0[s]}$ can be computed. The posterior-prior covariance difference $P_{k(+)} - P_{k(-)}$ in (22) becomes

$$P_{k(+)} - P_{k(-)} = -K_k H_k P_{k(-)} \quad (56)$$

which can be expressed in terms of S_k as

$$P_{k(+)} - P_{k(-)} = -P_{k(-)} S_k H_k P_{k(-)} \quad (57)$$

The priors on either side of (57) cancel with the inverses on

(51) when plugged into (22) yielding

$$P_{0[s]} = P_{0(+)} - \sum_{k=1}^N G_{k-1} \Phi_{k-1}^\top S_k H_k \Phi_{k-1} G_{k-1}^\top \quad (58)$$

as the improved forward update equation for the smoothed covariance $P_{0[s]}$. Finally, the ρ_k and τ_k termination criteria can now be re-considered in terms of G_{k-1} and S_k giving

$$\rho_k = \|G_{k-1} \Phi_{k-1}^\top S_k\| \quad (59)$$

$$\tau_k = \text{tr}(G_{k-1} \Phi_{k-1}^\top S_k H_k \Phi_{k-1} G_{k-1}^\top) / \text{tr}(P_{0[s]}^{[k]}) \quad (60)$$

This development directly leads to Algorithm 3—*efficient observed control*. The algorithm has a very similar computational burden to that of an EKF, with only one matrix inverse (guaranteed positive-definite symmetric) required each step. As in Algorithm 2, its forward-only structure also affords early termination when a sufficient horizon length is reached.

G. Separability into Reactive and Anticipatory

For linear-quadratic formulations such as (11), Algorithm 3 shows the recursive nature of the MPC update, which is linear in both the reference trajectory and the current state.

Theorem 3. *Assuming full-state feedback at the current time only, $H_0 = \mathbb{I}$, the linearity of the system can be used to factor the optimal predictive control policy into purely reactive and feed-forward anticipatory gain matrices where:*

1) *The sequence*

$$K_{eff} = G_{-1} S_0 + \sum_{k=1}^N G_{k-1} \Phi_{k-1}^\top S_k H_k \prod_{i=0}^{k-1} \Phi_i (\mathbb{I} - K_i H_i) \quad (61)$$

converges to the stabilizing LQR gain K_{lqr} as $N \rightarrow \infty$.

2) *The sequence for Λ_0 given by*

$$\Lambda_0 = - \sum_{k=1}^N G_{k-1} \Phi_{k-1}^\top S_k H_k \left(\prod_{i=1}^{k-1} \Phi_i (\mathbb{I} - K_i H_i) \right) \Phi_0 \quad (62)$$

3) *and the sequences for $\Lambda_1, \dots, \Lambda_N$ given by*

$$\Lambda_k = G_{k-1} \Phi_{k-1}^\top S_k - \sum_{j=k+1}^N G_{j-1} \Phi_{j-1}^\top S_j H_j \times \left(\prod_{i=k+1}^{j-1} \Phi_i (\mathbb{I} - K_i H_i) \right) \Phi_k K_k \quad (63)$$

converge to the optimal feed-forward anticipatory gains $\Lambda_0, \Lambda_1, \dots, \Lambda_N$, such that the control contribution $u_{a,n}$ resulting from the n^{th} target z_n is given by $u_{a,n} = \Lambda_n z_n$.

Proof. The forward dynamics of the prior states for the

observed system can be constructed from (5) as

$$x_{0(-)} = -r_0 + z_0 \quad (64a)$$

$$x_{1(-)} = -\Phi_0 (\mathbb{I} - K_0 H_0) r_0 + \Phi_0 z_0 \quad (64b)$$

$$x_{2(-)} = -\Phi_1 (\mathbb{I} - K_1 H_1) \Phi_0 (\mathbb{I} - K_0 H_0) r_0 + \Phi_1 (\mathbb{I} - K_1 H_1) \Phi_0 z_0 + \Phi_1 K_1 z_1 \quad (64c)$$

$$x_{k(-)} = - \left(\prod_{i=0}^{k-1} \Phi_i (\mathbb{I} - K_i H_i) \right) r_0 + \left(\prod_{i=1}^{k-1} \Phi_i (\mathbb{I} - K_i H_i) \right) \Phi_0 z_0 + \sum_{j=1}^{k-1} \left(\prod_{i=j+1}^{k-1} \Phi_i (\mathbb{I} - K_i H_i) \right) \Phi_j K_j z_j \quad (64d)$$

This then yields the sequence of residuals for $k = \{1, \dots, N\}$

$$r_k = z_k + H_k \left(\prod_{i=0}^{k-1} \Phi_i (\mathbb{I} - K_i H_i) \right) r_0 - H_k \left(\prod_{i=1}^{k-1} \Phi_i (\mathbb{I} - K_i H_i) \right) \Phi_0 z_0 - H_k \sum_{j=1}^{k-1} \left(\prod_{i=j+1}^{k-1} \Phi_i (\mathbb{I} - K_i H_i) \right) \Phi_j K_j z_j \quad (65)$$

Combining with (53), the expanded control is given by

$$u_{0[s]} = u_{0(+)} + \sum_{k=1}^N G_{k-1} \Phi_{k-1}^\top S_k \left\{ z_k + H_k \left(\prod_{i=0}^{k-1} \Phi_i (\mathbb{I} - K_i H_i) \right) r_0 - H_k \left(\prod_{i=1}^{k-1} \Phi_i (\mathbb{I} - K_i H_i) \right) \Phi_0 z_0 - H_k \sum_{j=1}^{k-1} \left(\prod_{i=j+1}^{k-1} \Phi_i (\mathbb{I} - K_i H_i) \right) \Phi_j K_j z_j \right\} \quad (66)$$

Using the relation $u_{0(+)} = u_{0(-)} + G_{-1} S_0 r_0$ and rearranging the last summation of (66) to group the z_k terms yields

$$u_{0[s]} = u_{\text{last}} + G_{-1} S_0 r_0 + \sum_{k=1}^N G_{k-1} \Phi_{k-1}^\top S_k H_k \left(\prod_{i=0}^{k-1} \Phi_i (\mathbb{I} - K_i H_i) \right) r_0 - \sum_{k=1}^N G_{k-1} \Phi_{k-1}^\top S_k H_k \left(\prod_{i=1}^{k-1} \Phi_i (\mathbb{I} - K_i H_i) \right) \Phi_0 z_0 + \sum_{k=1}^N \left[G_{k-1} \Phi_{k-1}^\top S_k - \sum_{j=k+1}^N G_{j-1} \Phi_{j-1}^\top S_j H_j \times \left(\prod_{i=k+1}^{j-1} \Phi_i (\mathbb{I} - K_i H_i) \right) \Phi_k K_k \right] z_k \quad (67)$$

where correspondence to the theorem subparts is directly observed. For regulators, all trajectory targets $\{z_0, \dots, z_N\}$ are trivially zero, leaving only the reactive components multiplied

by r_0 in (67). By Theorem 1, this zero-reference arrangement provides the optimal solution to the LQR regulation problem, which for the augmented system has the solution

$$u = u_{\text{last}} + K_{\text{lqr}} r_0 \quad (68)$$

where $u_{\text{last}} = u_{0(-)}$. Therefore, the K_{eff} sequence multiplying r_0 in (67) must converge to the infinite horizon LQR gain as $N \rightarrow \infty$. Further, given the equivalence between this control solution and the LQR problem in Theorem 1, the $\{\Lambda_0, \dots, \Lambda_N\}$ sequences must also converge to their optimal feed-forward anticipatory trajectory gains. \square

Corollary 3.1. *The convergence of the sequence (61) to K_{lqr} is monotonic and geometric in horizon length N .*

Proof. For each additional horizon step N , the change in K_{eff} is the difference $K_{\text{eff}}^{[N]} - K_{\text{eff}}^{[N-1]}$ which is given by

$$\Delta K_{\text{eff}} = G_{N-1} \Phi_{N-1}^\top S_N H_N \prod_{i=0}^{N-1} \Phi_i (\mathbb{I} - K_i H_i) \quad (69)$$

which after and using the definition (54a) becomes

$$\Delta K_{\text{eff}} = G_{N-1} \Phi_{N-1}^\top S_N H_N \Phi_{N-1} \prod_{i=0}^{N-1} (\mathbb{I} - K_i H_i) \Phi_{i-1} \quad (70)$$

Comparing to a similar $P_{0[s]}^{[N]} - P_{0[s]}^{[N-1]}$ treatment of (58) and noting that the product in (70) is nearly G_{N-1}^\top in (54c) yields

$$\Delta P_{0[s]} = -\Delta K_{\text{eff}} P_{0(-)} \begin{bmatrix} 0 & \mathbb{I} \end{bmatrix}^\top \quad (71)$$

Since additional future information can only reduce initial uncertainty, $P_{0[s]}$ must converge monotonically, that is $\Delta P_{0[s]}$ must be negative semi-definite. Therefore, as $P_{0(-)}$ is positive definite it cannot change the sign of ΔK_{eff} and the difference $\|K_{\text{lqr}} - K_{\text{eff}}\|$ must converge to zero monotonically. \square

Corollary 3.2. *For some positive constant $\gamma > 0$, the convergence error $\|K_{\text{lqr}} - K_{\text{eff}}\| < \gamma \text{tr}(\Delta P_{0[s]})$ as $N \rightarrow \infty$.*

Proof. In the proof of Corollary 3.1, it is shown that $\Delta P_{0[s]} = -\Delta K_{\text{eff}} P_{0(-)} \begin{bmatrix} 0 & \mathbb{I} \end{bmatrix}^\top$. Thus, the convergence rates are the same between K_{eff} and $P_{0[s]}$ within a factor γ . The rate of convergence is geometric in the square eigenvalues of the closed-loop system $(\mathbb{I} - K_i H_i) \Phi_{i-1}$, which for large N becomes the closed-loop infinite-time Kalman system $(\mathbb{I} - K_\infty H) \Phi$, which by Theorem 2 has all eigenvalues within the unit circle. Thus, the convergence errors are bounded by

$$\|K_{\text{lqr}} - K_{\text{eff},N}\| < \gamma_k \sum_{n=N}^{\infty} \lambda_{\text{max}}^{2n} \quad (72a)$$

$$< \gamma_k \frac{\lambda_{\text{max}}^{2N}}{1 - \lambda_{\text{max}}^2} \quad (72b)$$

$$\|P_{0[s],\infty} - \sum_{n=N}^{\infty} \Delta P_{0[s],n}\| < \gamma_p \sum_{n=N}^{\infty} \lambda_{\text{max}}^{2n} \quad (72c)$$

$$< \gamma_p \frac{\lambda_{\text{max}}^{2N}}{1 - \lambda_{\text{max}}^2} \quad (72d)$$

where λ_{max} is the maximum magnitude (controllable) eigenvalue of the closed-loop Kalman system. The error $\|K_{\text{lqr}} - K_{\text{eff}}^{[N]}\|$ and initial covariance $P_{0,[s]}$ both converge quadratically with N and differ by the factor $\gamma = \gamma_k/\gamma_p$. Therefore, the early termination metric $\tau = \text{tr}(\Delta P_{0[s]}/P_{0[s]})$ is equivalent to $\|K_{\text{lqr}} - K_{\text{eff}}^{[N]}\| < \epsilon \|K_{\text{lqr}}\|$ for some ϵ . \square

Remark. *Given (72b), an approximation for the horizon length N , given a desired convergence tolerance ϵ such that*

$$\epsilon \approx \frac{\|K_{\text{lqr}} - K_{\text{eff}}\|}{\|K_{\text{lqr}}\|} \quad (73)$$

is given from the geometric series as

$$N \approx \frac{\log(\epsilon)}{2 \log(\lambda_{\text{max}})} \quad (74)$$

However, since the convergence of K_{eff} is not purely geometric until large N , this only acts in practice as a heuristic for the termination criteria used in the algorithms and K_{eff} convergence to a ratio of ϵ .

Corollary 3.3. *Given a controllable linear system with quadratic costs, there exists a finite horizon N such that the anticipatory feed-forward effect of including additional information available from an infinite horizon Lipschitz continuous trajectory falls below any desired value ϵ , that is*

$$\|u_\infty - u_N\| < \epsilon \text{ if } \|z_k - z_{k-1}\| < \delta \forall k > N. \quad (75)$$

Proof. The complete control update for an infinite horizon can be expressed by Theorem 3 as

$$\begin{aligned} u_\infty &= u_{\text{last}} + K_{\text{lqr}} r_0 + \Lambda_0 z_0 + \Lambda_1 (z_0 + z_1 - z_0) + \{\dots\} \\ &= u_{\text{last}} + K_{\text{lqr}} r_0 + \Lambda_0 z_0 + \Lambda_1 (z_0 + \Delta z_1) + \{\dots\} \\ &= u_{\text{last}} + K_{\text{lqr}} r_0 + \sum_{n=0}^{\infty} \Lambda_n z_0 + \sum_{n=1}^{\infty} \left(\sum_{m=n}^{\infty} \Lambda_m \right) \Delta z_n \end{aligned} \quad (76)$$

Thus, control difference $u^{[\infty]} - u^{[N]}$ is given by

$$u_\infty - u_N = \sum_{n=N+1}^{\infty} \left(\sum_{m=n}^{\infty} \Lambda_m \right) \Delta z_n \quad (77)$$

Applying the triangle inequality to (77) yields the inequality

$$\|u_\infty - u_N\| \leq \sum_{n=N+1}^{\infty} \left(\sum_{m=n}^{\infty} \|\Lambda_m\| \right) \|\Delta z_n\| \quad (78)$$

The norm of each Λ_m term, defined in (63), is bounded by

$$\begin{aligned} \|\Lambda_m\| &\leq \|G_{m-1} \Phi^\top S_m\| \\ &+ \sum_{i=m}^N \left\| G_{i-1} \Phi^\top S_i H \Phi \left(\prod_{k=m+1}^i (\mathbb{I} - K_{k-1} H) \Phi \right) K_i \right\| \end{aligned} \quad (79)$$

having again applied the triangle inequality. Using the fact that

$$\|\Phi_{i-1}^\top (\mathbb{I} - K_i H)^\top\| \leq \lambda_{\text{max}} \quad (80)$$

and the multiplicative property of norms, (79) becomes

$$\|\Lambda_n\| \leq \gamma_1 \lambda_{\text{max}}^m + \sum_{i=m}^{\infty} (\lambda_{\text{max}}^i) \gamma_2 (\lambda_{\text{max}}^{i-m}) \quad (81)$$

noting the presence of (80) in the G terms given by (54c) and defining $\gamma_1 = \|\Phi^\top S_n\|$ and $\gamma_2 = \|\Phi^\top S_i H \Phi\| \|K_i\|$. Thus,

$$\|\Lambda_m\| \leq \gamma_1 \lambda_{max}^m + \gamma_2 \lambda_{max}^{2m} \sum_{i=0}^{\infty} \lambda_{max}^{2i} \quad (82)$$

$$\leq \gamma_1 \lambda_{max}^m + \frac{\gamma_2 \lambda_{max}^{2m}}{1 - \lambda_{max}^2} \quad (83)$$

noting the change in the summation range of (82). Plugging the result (83) into (78) and applying the triangle inequality and summation property used in (82) yields the result

$$\|u_\infty - u_N\| \leq \left(\frac{\gamma_1 \lambda_{max}^{N+1}}{(1 - \lambda_{max})^2} + \frac{\gamma_2 \lambda_{max}^{2(N+1)}}{(1 - \lambda_{max}^2)^3} \right) \delta \quad (84)$$

which completes the proof as the terms of (84) will approach 0 as $N \rightarrow \infty$ since λ_{max} is guaranteed to be within the unit circle ($|\lambda_{max}| < 1$) by Theorem 2 for a controllable system. However, if the system passes through an uncontrollability, the eigenvalues appear on the unit circle ($|\lambda_{max}| = 1$) for those horizon steps, and additional look-ahead is required. \square

Theorem 4. *The anticipatory control contribution of a prediction horizon u_a can be computed independently of the current state based on the current and upcoming references $\{z_0, \dots, z_N\}$. This anticipatory component can be added to a purely reactive K_{lqr} control law, enabling any-time any-horizon MPC and computed using the same Kalman filtering recursions. This yields the control policy*

$$u_0 = K_{lqr} r_0 + \sum_{k=0}^N u_{a,k} \quad (85)$$

which enables any-time termination of the algorithm, while ensuring at minimum LQR's stability and performance.

Proof. To compute the anticipatory control contribution using only $\{z_0, \dots, z_N\}$, initialize the Kalman filter with $x_{0(-)} = z_0$. Then the first residual is $r_0 = 0$, which removes the current state-error feedback already handled by K_{lqr} and yields the sequence of z_0 -relative residuals given by

$$\begin{aligned} r_k = z_k - H_k \left(\prod_{i=1}^{k-1} \Phi_i (\mathbb{I} - K_i H_i) \right) \Phi_0 z_0 \\ - H_k \sum_{j=1}^{k-1} \left(\prod_{i=j+1}^{k-1} \Phi_i (\mathbb{I} - K_i H_i) \right) \Phi_j K_j z_j \end{aligned} \quad (86)$$

for $k \in [1, N]$. Combining (86) with the efficient algorithm's summation (53) yields the anticipatory control contribution identical to that of (67) in the proof of Theorem 3 without the terms multiplied by r_0 . Therefore, with the initialization of $x_{0(-)} = z_0$, the same forward-only approach as Algorithm 3 computes the anticipatory control contribution sum u_a for any horizon N independent of the current system state error. \square

Algorithm 4—any-time any-horizon observed control—follows directly from Theorem 4, which establishes that anticipatory control contributions can be computed independently of the current state. It parallels Algorithm 3, but with the key

Algorithm 4 Any-Time Any-Horizon Observed Control

initialize $P_{0(-)} \leftarrow \dot{Q}$, $G_{-1} \leftarrow [\mathbb{O} \quad \mathbb{I}] \dot{Q}$
 $\text{tr}(P_{0[s]}) \leftarrow \text{tr}(P_{0(-)})$, $\chi_{0(-)} \leftarrow z_0$, $u_a \leftarrow \mathbf{0}$

for $k \in [0, \dots, N]$ **do** ▷ Single Forward Pass
if $k > 0$ **then**
 $\chi_{k(-)} \leftarrow \Phi_{k-1} \chi_{k-1(+)} \quad \triangleright (5a)$
 $P_{k(-)} \leftarrow \Phi_{k-1} P_{k-1(+)} \Phi_{k-1}^\top + \dot{Q}_{k-1} \quad \triangleright (5b)$
 $r_k \leftarrow z_k - H_k \chi_{k-1(-)} \quad \triangleright (5c)$
 $S_k = H_k^\top [H_k P_{k(-)} H_k^\top + \dot{R}_k]^{-1} \quad \triangleright \text{Only Inverse (54e)}$
 $K_k = P_{k(-)} S_k \quad \triangleright (55)$
 $\chi_{k(+)} \leftarrow \chi_{k(-)} + K_k r_k \quad \triangleright (5d)$
 $P_{k(+)} \leftarrow [\mathbb{I} - K_k H_k] P_{k(-)} \quad \triangleright (5e)$

$\Psi_k \leftarrow G_{k-1} \Phi_{k-1}^\top S_k H_k \Phi_{k-1} G_{k-1}^\top \quad \triangleright \Delta P_{0[s]}$
 $u_a \leftarrow u_a + G_{k-1} \Phi_{k-1}^\top S_k r_k \quad \triangleright (53)$
 $\text{tr}(P_{0[s]}) \leftarrow \text{tr}(P_{0[s]}) - \text{tr}(\Psi_k) \quad \triangleright (58)$

$\rho_k \leftarrow \|G_{k-1} \Phi_{k-1}^\top S_k\| \quad \triangleright (59)$
 $\tau_k \leftarrow \text{tr}(G_{k-1} \Phi_{k-1}^\top S_k H_k \Phi_{k-1} G_{k-1}^\top) / \text{tr}(P_{0[s]}) \quad \triangleright (60)$
if $\rho \leq \delta_1$ **and** $\tau_k \leq \delta_2$ **break** ▷ Early Termination

$G_k = G_{k-1} \Phi_{k-1}^\top (\mathbb{I} - K_k H_k)^\top \quad \triangleright (54d)$

return $u_{\text{last}} + K_{lqr}(z_0 - H_0 \chi_0) + u_a$

initialization difference of $x_{0(-)} = z_0$. Separately, the infinite-time K_{lqr} gain is applied to the current error, guaranteeing at worst, the stability and performance of LQR. Furthermore, the forward pass may be terminated at any point while preserving these guarantees, thereby motivating the algorithm's name.

Remark. *Theorem 3 proves that linear-quadratic MPC is the superposition of a reactive and anticipatory component. Theorem 4 proves that anticipatory controls u_a do not require any state information and can therefore be precomputed and tabulated for the entire trajectory using Algorithm 4.*

H. Extensions to Nonlinear Systems

While the proposed algorithms use the Kalman filter and RTS smoother, observed control is compatible with any estimator allowing zero process noise to enforce the dynamics constraints. Addressing systems where the dynamics (2b) are nonlinear is accomplished with a nonlinear filter extension, e.g. EKF or UKF; for details, the reader is referred to [41], [48]. For EKF, the augmented state-sensitivity matrix becomes

$$\Phi_k = \begin{bmatrix} \mathcal{F}_x & \mathcal{F}_u \\ 0 & \mathbb{I}_m \end{bmatrix} \quad (87)$$

where $\mathcal{F}_x = \frac{\partial f(x_{k-1}, u_{k-1})}{\partial x_{k-1}}$ and $\mathcal{F}_u = \frac{\partial f(x_{k-1}, u_{k-1})}{\partial u_{k-1}}$ are the one-step state and control sensitivity matrices. These can be found by simultaneous integration of the system dynamics, state sensitivity, and control sensitivity equations given by

$$\dot{x} = g(x, u) \quad \dot{\mathcal{F}}_x = \frac{\partial g}{\partial x} \mathcal{F}_x \quad \dot{\mathcal{F}}_u = \frac{\partial g}{\partial x} \mathcal{F}_u + \frac{\partial g}{\partial u} \quad (88)$$

with the initial conditions x_{k-1} , \mathbb{I} and \mathbb{O} , respectively.

I. Extensions to Nonquadratic Objective Functions

The Kalman filter to LQR duality guides the mapping of quadratic objective functions of state and control. As shown in Theorem 1, LQR costs invert to become filter covariances (12), blocked to align with the augmented state (9). If penalizing every state and control, $H_k = \mathbb{I}$ (13) and the residual r_k is given by (15). To not penalize specific states or controls, drop the appropriate rows of H_k , thus not measuring them in the filter. The existence of costing in both the measurement H_k and residual r_k makes extension to nonquadratic costs nuanced, for which both SQP-like and gradient-based methods are presented. To use these methods in any algorithm, simply replace the appropriate measurement equations for the desired measurement mode as summarized in Table I.

1) *SQP-Based Measurement*: First, consider the standard LQR cost function (11a) already discussed, but for simplicity without the control change penalty,

$$J = \sum \frac{1}{2} \chi_k^\top \begin{bmatrix} Q_{[\text{lqr}]} & M_{[\text{lqr}]} \\ M_{[\text{lqr}]}^\top & R_{[\text{lqr}]} \end{bmatrix} \chi_k \quad (89)$$

when expressed with augmented state. The first-order optimality residual and its sensitivity at each update are given by

$$\frac{\partial J}{\partial \chi_k} = \begin{bmatrix} Q_{[\text{lqr}]} & M_{[\text{lqr}]} \\ M_{[\text{lqr}]}^\top & R_{[\text{lqr}]} \end{bmatrix} \chi_k \quad \frac{\partial^2 J}{\partial \chi_k^2} = \begin{bmatrix} Q_{[\text{lqr}]} & M_{[\text{lqr}]} \\ M_{[\text{lqr}]}^\top & R_{[\text{lqr}]} \end{bmatrix} \quad (90)$$

Correspondence to the Kalman filter equations (5f) and (5d) implies the optimal residual, sensitivity, and noise are

$$r_k = \left(\frac{\partial^2 J}{\partial \chi_k^2} \right)^{-1} \frac{\partial J}{\partial \chi_k} \quad (91)$$

$$H_k = \left(\frac{\partial^2 J}{\partial \chi_k^2} \right)^{-1} \frac{\partial^2 J}{\partial \chi_k^2} = \mathbb{I} \quad (92)$$

$$\dot{R}_k = \left(\frac{\partial^2 J}{\partial \chi_k^2} \right)^{-1} \quad (93)$$

Therefore, the optimal anticipated residual for a quadratic objective is a single quadratic-programming update, with a full-state identity measurement sensitivity H_k and inverse hessian as the measurement noise. Thus, the observed control measurement residual represents the change in states and controls necessary to optimize each horizon step individually. Extension to nonlinear scalar objective functions directly follows. In each step, the residual is the state change necessary to realize the first-order optimality criterion and the measurement noise is the inverse Hessian—which must be positive definite for a minimum by the second-order optimality criterion. Just as in nonlinear SQP solvers, if the Hessian is rank deficient, a symmetry-preserving pseudo-inverse should be used.

2) *Gradient-Based Measurement*: Often it is more natural to express the desired anticipated residual, i.e., regret, r_k directly or heuristically, instead of explicitly as the derivative of a scalar function. This is advantageous as it is often easier to define a relative *which way is better* ($\frac{\partial J}{\partial \chi}$) rather than an *exactly how bad is it* (J). Thus, in general, residuals can be

	Duality-Based Measurement (a)	One-Step SQP Measurement (b)	Gradient-Based Measurement (c)
Residual	$r_k = z_k - \hat{\chi}_k$ (15)	$r_k = \frac{\partial^2 J}{\partial \chi_k^2}^\dagger \frac{\partial J}{\partial \chi_k}$ (91)	$r_k = \frac{\partial J}{\partial \chi_k}$ (94)
Sensitivity	$H_k = \mathbb{I}_\eta$ (13)	$H_k = \frac{\partial^2 J}{\partial \chi_k^2}^\dagger \frac{\partial^2 J}{\partial \chi_k^2}$ (92)	$H_k = \frac{\partial^2 J}{\partial \chi_k^2}$ (95)
Covariance	$\dot{R}_k = \begin{bmatrix} Q & M \\ M^\top & R \end{bmatrix}^{-1}$ (12)	$\dot{R}_k = \frac{\partial^2 J}{\partial \chi_k^2}^\dagger$ (93)	$\dot{R}_k = \alpha \mathbb{I}_\eta$ (96)

TABLE I: Observed control measurement modes for quadratic (a) and nonquadratic (b, c) objectives.

incorporated in the same guise as the EKF, where

$$r_k = r(\chi_{k(-)}) \quad (94)$$

$$H_k = \frac{\partial r(\chi_{k(-)})}{\partial \chi_{k(-)}} \quad (95)$$

$$\dot{R}_k = \alpha \mathbb{I} \quad (96)$$

The parameter α behaves like the step size in gradient descent for the criterion weight \dot{R}_k . The first-order optimality criterion $r_k = 0$ must still be satisfied for the generic heuristic function $r(\chi_{k(-)})$ when the system is at the desired condition. Implicitly, this still optimizes some scalar objective; however, the exact objective need not be explicitly represented. This approach is also advantageous when implementing within the UKF framework, as the inverse Hessian is not required.

IV. CASE STUDIES AND DISCUSSION

A. Linear-Quadratic MPC with Observed Control

A classic mass-spring-damper (MSD) system, with dynamics $m\ddot{x} + b\dot{x} + kx = F_u$ where $m = 1$, $b = 1$, and $k = 2$ serves as a benchmark for evaluating the reactive, predictive, and anytime variants of observed control. The MPC objective is chosen to be the LQR cost function (11a) with weights

$$Q_{[\text{lqr}]} = \begin{bmatrix} 10 & 0 \\ 0 & 1 \end{bmatrix} \quad R_{[\text{lqr}]} = \begin{bmatrix} 0.1 \\ 0.1 \end{bmatrix} \quad M_{[\text{lqr}]} = \begin{bmatrix} 0 \\ 0 \end{bmatrix} \quad (97)$$

Figure 1 compares Algorithms 1-4 performing step inputs for various time horizon lengths N , with a discrete LQR controller baseline; all $\Delta t = 0.1$. The discrete LQR control law is

$$u_{\text{lqr}} = -K_{\text{lqr}} x_{\text{ref}} + u_{ss} \quad (98)$$

where $u_{ss} = B^\dagger(\mathbb{I} - A)x_{\text{ref}}$ compensates for steady-state error caused by penalizing control effort. This term ensures convergence to steady state by solving $x_{\text{ref}} = Ax_{\text{ref}} + Bu_{ss}$ at the desired equilibrium x_{ref} . In observed control, the same behavior is achieved by making the measurement H_k

$$H_k = [\mathbb{I}_{n \times n} \quad \mathbb{O}_{n \times m}] \quad (99)$$

which removes any control penalty. Observed control's u_{ss} is provided by the predictive time horizon, but remains bounded by the Δu penalty, ensuring no integrator windup effects.

Figure 1a shows reactive step responses of Algorithms 1-3, without trajectory anticipation, see Section III-A, for various horizon lengths N . As expected, performance improves with larger N , ultimately converging to that of LQR, consistent with Theorem 1. Figure 1b shows predictive responses for Algorithms 1-3, where larger N enables the controllers to optimally

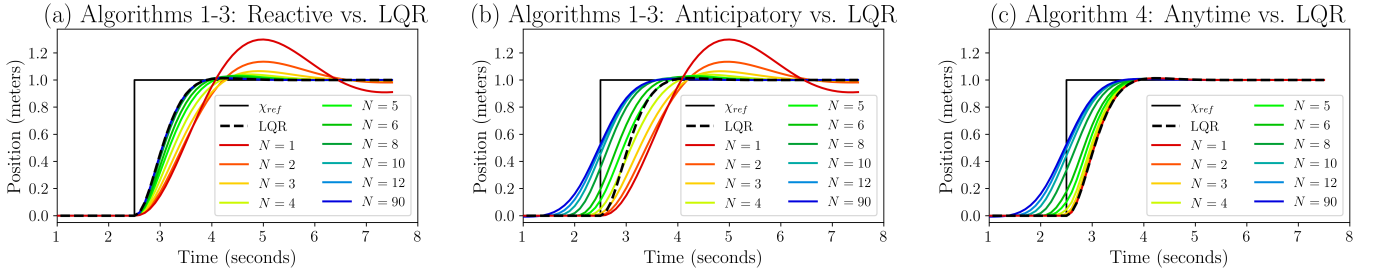


Fig. 1: Step responses of Algorithms 1-4 ($\Delta t = 0.1$) in reactive (1a), predictive (1b), and any-time any-horizon (1c) modes. Without trajectory anticipation, Algorithms 1-3 converge to the optimal discrete LQR solution; with anticipation, all converge to the predictive optimal, with Algorithm 4 achieving the reactive optimal with $N = 0$.

anticipate and center the step. Algorithm 4, the any-time any-horizon variant, shown in Figure 1c, decomposes the horizon into purely reactive and anticipatory components, ensuring LQR's optimal reactive behavior for $N = 0$, with predictive performance improving monotonically as N increases.

Figure 2 presents the integrated cost on a continuous plant

$$C = \int_{t=0}^{7.5} \left(\chi_k^\top \begin{bmatrix} Q_{[lqr]} & M_{[lqr]} \\ M_{[lqr]}^\top & R_{[lqr]} \end{bmatrix} \chi_k + \|u_k - u_{k-1}\|_{R_{[lqr]}}^2 \right) dt \quad (100)$$

with weights (97) for each algorithm across various horizon lengths N . All controllers stabilize the system with no steady-state error, resulting in bounded accumulated costs. Algorithms 1-3 converge to the reactive optimum by $N = 10$ whereas Algorithm 4 begins at the reactive optimum with $N = 0$, highlighting its advantage in short-horizon settings. By $N = 12$, all algorithms converge to the predictive control optimum.

All algorithms demonstrate convergence to the predictive control optimum; however, the key contribution lies in Algorithm 4 and its guaranteed baseline performance. It closes the gap for short time horizons, ensuring at worst LQR performance and stability, guaranteeing that there is always a reasonable stabilizing control ready while using any remaining compute time between updates for refinement.

B. Non-Quadratic Costs and Measurement Modes

Quadratic objectives have well-defined minima; however, they limit the types of behavior that can be encoded into a MPC controller. Section III-I presents SQP-like and gradient-based methods for incorporating nonquadratic objectives into observed control. Table I summarizes the construction of measurement residuals, sensitivities, and covariances for the nonquadratic case, which are equivalent to the duality-based formulation when the objective function is itself quadratic.

To illustrate the behavior of different measurement modes under nonquadratic objectives, consider the 2D linear system with integrator dynamics and drag, termed the linear drag system, governed by the dynamics

$$m \begin{bmatrix} \ddot{x} \\ \ddot{y} \end{bmatrix} + b \begin{bmatrix} \dot{x} \\ \dot{y} \end{bmatrix} = \begin{bmatrix} F_x \\ F_y \end{bmatrix} \quad (101)$$

with $m = 1$ and $b = 1$. The controller is tasked with tracking a full-state reference trajectory χ_{ref} while also avoiding reference-intersecting obstacles. The augmented state χ is

$$\chi = \begin{bmatrix} x & y & \dot{x} & \dot{y} & F_x & F_y \end{bmatrix}^\top \quad (102)$$

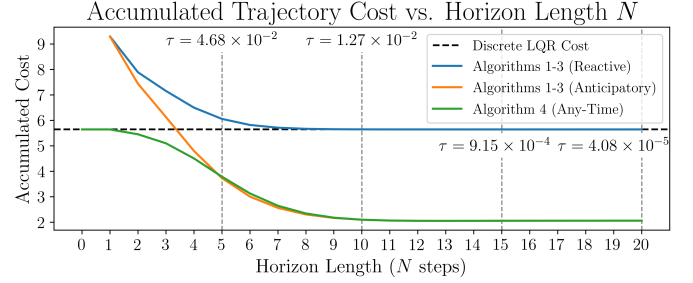


Fig. 2: Integrated trajectory costs for each observed control algorithm vs. horizon length N . All algorithms converge to the predictive optimal as N increases with trajectory anticipation, with Algorithm 4 starting at the reactive optimal with $N = 0$.

which is penalized by W_χ . To impose obstacle avoidance, the obstacle potential field cost $\mathcal{C}(d)$ is introduced, given by

$$\mathcal{C}(d) = 0.01 \left(\frac{2 \cdot d_z}{\pi(d - d_z)} \tan \left(\frac{\pi(d - d_z)}{2 \cdot d_z} \right) - 1 \right) \quad (103)$$

where $d(\chi)$ is the minimum distance to obstacle and $d_z = 0.5$ specifies the zero-cost distance. As $d \rightarrow 0$, $\mathcal{C} \rightarrow \infty$, ensuring collision avoidance. The combined objective function is

$$J = \frac{1}{2} \sum_{k=0}^N (\|\chi_k - \chi_{ref}\|_{W_\chi}^2 + W_o \mathcal{C}(d)) \quad (104)$$

where the two objective weights $W_\chi = \text{diag}([100, 1, 0.1, 0.1])$ and $W_o = 20000$. The controllers are expected to minimize the reference trajectory tracking error while avoiding collisions. Figure 3 illustrates the behaviors resulting from the SQP-like and gradient-based ($\alpha = 1, 2, 4, 8, 32$) measurement modes.

The SQP-like measurement mode is the preferred method for optimizing scalar objective functions like (104) in the way optimal control problems are traditionally set up. Combining the Kalman gain (5f) and posterior state update (5d) with the SQP-like measurement yields the posterior-prior difference

$$\tilde{\chi}_k = P_{k(-)} \left[P_{k(-)} + \left(\frac{\partial^2 J}{\partial \chi_k^2} \right)^{-1} \right]^{-1} r_k \quad (105)$$

where $\tilde{\chi}_k = \chi_{k(+)} - \chi_{k(-)}$. Each step, these $\tilde{\chi}_k$ differences map through smoother gains to become control refinements and (105) highlights how the ratio between the covariance $P_{k(-)}$ and cost-to-go dual $(\partial^2 J / \partial \chi_k^2)^{-1}$ weight the residual direction r_k . The aggregate measurement mode with its SQP

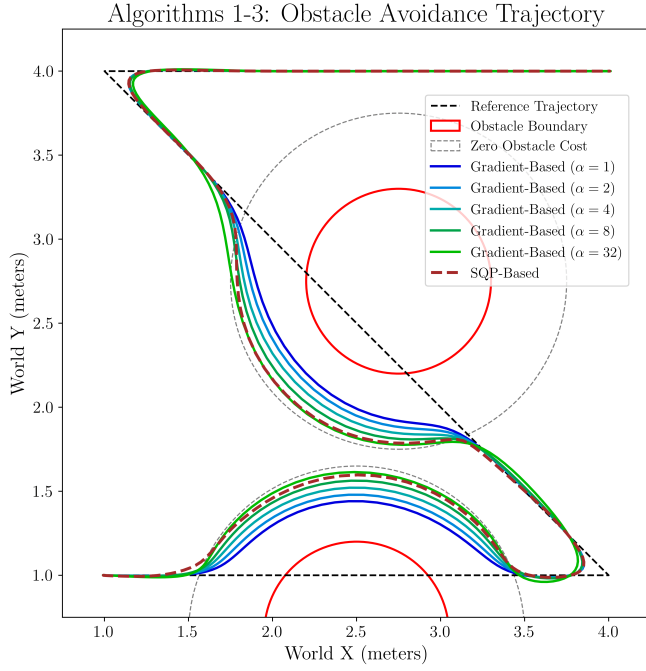


Fig. 3: Observed control performing obstacle avoidance on a collision-containing trajectory with a nonquadratic cost function on the linear drag system (101). The SQP-like mode finds the locally optimal trajectory while the gradient-based mode with various α values demonstrates the tunability of *direction-to-better* objectives.

heritage effectively finds the local minima between encroaching on the obstacles and deviating from the trajectory.

However, when tuning an MPC controller, it is often easier to describe a *direction to better* ($\partial J / \partial x_k$) and *how much to care* weight α for which gradient-based measurements provide for a more intuitive interface. In the gradient framework, the objective function is instead a vector of gradients with weights

$$\frac{\partial J}{\partial \mathbf{x}} = \begin{bmatrix} \chi_{k, err} \\ \frac{\partial \mathcal{C}}{\partial \mathbf{x}} \end{bmatrix} \quad \dot{\mathbf{R}} = \alpha \begin{bmatrix} \mathbf{W}_x^{-1} & 0 \\ 0 & \mathbf{W}_o^{-1} \end{bmatrix} \quad (106)$$

and the posterior-prior difference is given by

$$\tilde{\chi}_k = P_{k(-)} \frac{\partial^2 J}{\partial \mathbf{x}_k^2}^\top \left[\frac{\partial^2 J}{\partial \mathbf{x}_k^2} P_{k(-)} \frac{\partial^2 J}{\partial \mathbf{x}_k^2}^\top + \dot{\mathbf{R}} \right]^{-1} r_k \quad (107)$$

where α can be intuited as a gradient descent step size in the ratio of how r_k maps to control refinements. Figure 3 shows the gradient-based method approaching the SQP-like path as α initially increases; however, further increasing α makes for a wider avoidance instead of convergence to the SQP-like path.

This example outlines the key differences between the non-quadratic measurement modes. The SQP-like method performs Newton steps towards minimizing the scalar objective (105), maintaining a fixed measurement size of η . In contrast, the gradient-based method supports a broader class of objectives and behaviors—including those without an analytical $J(\mathbf{x})$, those impractical to directly evaluate, or those incorporating learned objectives or heuristics—and offers greater tunability. While the SQP-like method is computationally advantageous, the gradient-based method's flexibility comes at the cost of a potentially larger measurement size and $\dot{\mathbf{R}}$ inversion.

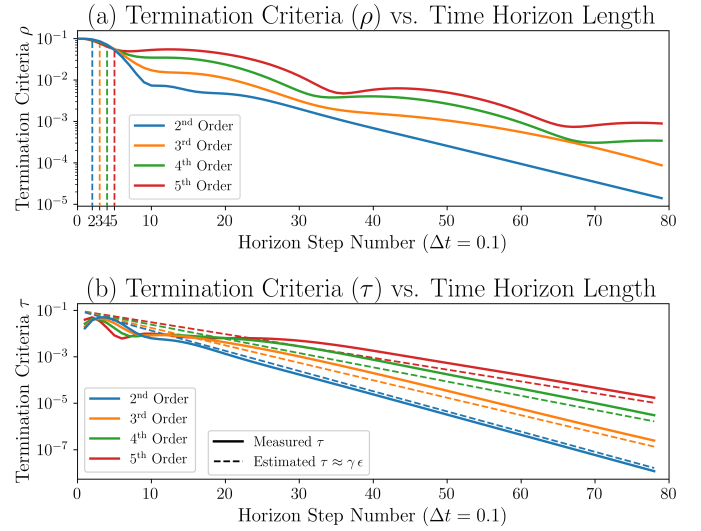


Fig. 4: The ρ and τ with ($\gamma = 0.1$) early termination criteria vs horizon step number N for various order linear systems. Notably, the accumulator gain criteria ρ peaks when the system first becomes fully controllable. The τ estimate is found by rearranging (74).

C. Early Termination (Algorithms 2-4)

The key feature of Algorithms 2-4 is their single forward-only structure, iterating through horizon steps sequentially into the predictive horizon. This structure enables the controllers to precisely quantify the additional control refinement on u_0 resulting from extending the predictive horizon length from N to $N + 1$, via the termination metrics ρ and τ introduced in Section III-E. These metrics can be precomputed for linear systems or evaluated on-the-fly using repeated linearizations and the filter's covariances for nonlinear systems enabling adaptive horizon length selection and early termination of the MPC optimization without sacrificing control performance.

Figure 4 illustrates both termination criteria as a function of the horizon length N for several representative linear systems. Each n -th order system was constructed with the first n poles chosen from the set $\mathcal{P} = \{-0.1, -0.2, -0.3, -0.4, -0.5\}$ with the system matrices A and B defined as

$$A = \begin{bmatrix} \vec{0}_{n-1} & \mathbb{I}_{n-1} \\ [-a_0 & -a_1 & \cdots & -a_{n-1}] \end{bmatrix} \quad B = \begin{bmatrix} \vec{0}_{n-1} \\ 1 \end{bmatrix} \quad (108)$$

where $\{a_0, a_1, \dots, a_{n-1}\}$ are the coefficients of the characteristic polynomial defined by the chosen poles. This construction ensures each system's controllability index matches its order.

As shown in Figure 4a, the accumulator gain norm-based criteria ρ initially grows and peaks as the horizon length N reaches the system's controllability index, reflecting full controllability of the state. Beyond this point, ρ decreases as additional future-time horizon steps have diminishing influence on u_0 . Small periodic dips appear after controllability is established and repeat thereafter, corresponding to the natural harmonics in the augmented system Φ , which are also reflected in the accumulators Γ_k and G_k used in finding ρ . Similarly, Figure 4b shows the uncertainty metric τ and the horizon estimation heuristic (74) as a function of N . For this system, the scaling factor for $P_{\infty[s]}/K_\infty$ convergence ratio

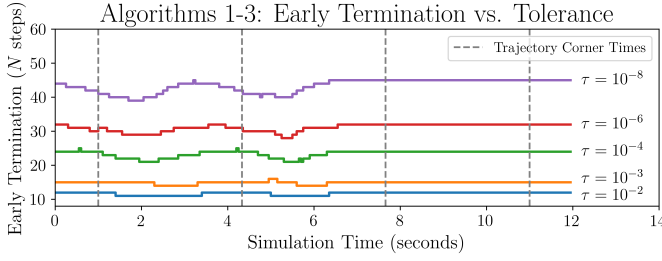


Fig. 5: Terminated horizon lengths for the obstacle avoidance scenario (gradient-based measurement mode) for various τ convergence thresholds. Vertical lines indicate scheduled trajectory corners.

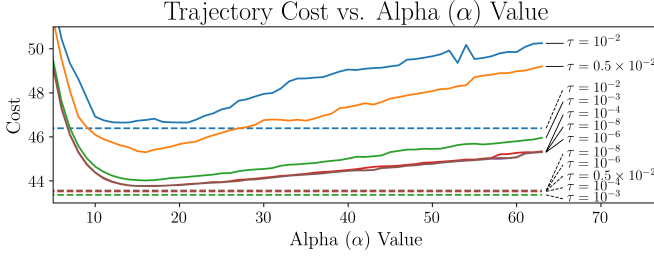


Fig. 6: Trajectory cost ratios for various τ convergence thresholds (gradient-based measurement) across different α values. As the threshold for τ is tightened, the curves converge for all α values. The dotted color-matched lines are the SQP-based mode for each τ .

was empirically determined to be $\gamma \approx 0.1$. Here, the transient τ -dynamics are captured early, and τ exhibits geometric (exponential) convergence consistent with the heuristic (74). This confirms that the controllers rapidly achieve the minimum horizon length required to sufficiently approximate the infinite-horizon u_0 under a stationary reference trajectory.

For the obstacle avoidance problem with the linear drag system, Figure 5 shows the resulting adaptive horizon lengths selected throughout the entire simulation as the system is controlled from the lower left corner to the upper right corner. The gradient-based measurement is used, and the ρ metric ignored to isolate the effects of τ as references are known smooth. As the cost gradient becomes better defined, particularly near obstacles, the number of horizon steps required to reach a given control confidence tolerance decreases. Predictably, tightening the tolerance increases the average number of required horizon steps, but the curve retains its general shape.

Figure 6 plots the accumulated objective costs of the linear drag system obstacle avoidance problem for various $\tau \leq \delta_1$ convergence tolerances with respect to (104). Note that the resulting trajectories effectively converge when $\tau \approx 10^{-3}$. The solid curves correspond to the entire range of α values in the gradient-based measurement mode, while the dotted, color-matched lines indicate the corresponding SQP-based cost at the same τ tolerance. As the τ threshold is tightened, the costs converge to their respective optima across all α values. The residual difference between the gradient-based and SQP-based costs reflects the inherent differences between gradient and SQP step directions when optimizing a nonquadratic objective. The observed jitter in the curves arises from the discrete nature of N and its interaction with the τ thresholds.

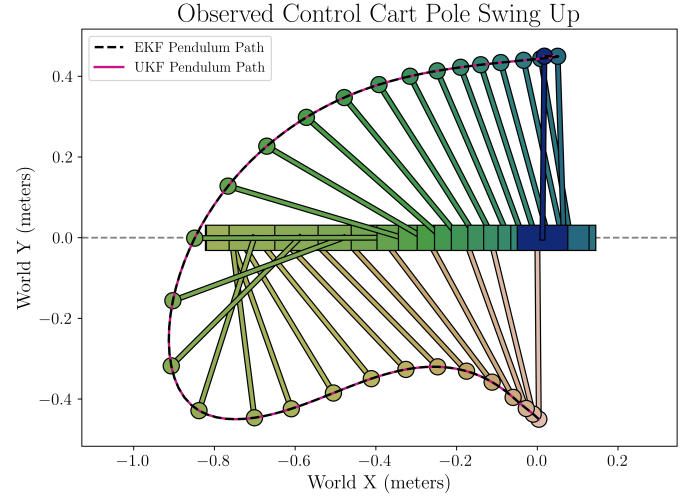


Fig. 7: Example cart pole swing-up performed by observed control (Algorithm 2, backend EKF), with the gradient measurement mode ($\alpha = 1$). The UKF-backend trajectory is effectively indistinguishable.

Even for linear systems, selecting an appropriate horizon is difficult; for nonlinear systems, nonquadratic objectives, or nonstationary trajectories, the difficulty compounds. Observed control quantifies tradeoffs in horizon length, closed-loop performance, and computational complexity. Corollary 2.1 and 2.2 emphasize the importance of jointly considering both convergence to an infinite-time approximation and impact of reference trajectory changes, while Corollary 3.3 connects horizon selection to reference trajectory smoothness. By quantifying, at runtime, the incremental refinement in u_0 from each additional horizon step, observed control enables the dynamic determination of min-length horizons, making it particularly suitable for complex control problems.

D. Non-Linear Cart Pole Swing Up

Figure 7 shows observed control performing a cart-pole swing up — a widely used benchmark for nonlinear predictive control. In this experiment, force control was applied to the cart's horizontal axis, and the pole is modeled as a weightless rigid link with all the mass concentrated at the endpoint. The augmented state χ for the system is defined as

$$\chi = [x \quad v \quad \theta \quad \omega \quad F_x]^\top \quad (109)$$

where x is the cart's horizontal position, $v = \dot{x}$ is the cart's horizontal velocity, θ is the pole angle relative to the vertical (counter-clockwise positive), $\omega = \dot{\theta}$ is the angular velocity of the pole, and F_x is the control input force applied to the cart. The nonlinear dynamics of the system are given by

$$\ddot{x} = [l(m_p \sin^2 \theta + m_c)]^{-1} [lF_x - d_v l \dot{x} - m_p l^2 \dot{\theta}^2 \sin \theta - (d_\omega \dot{\theta} - g m_p l \sin \theta) \cos \theta] \quad (110a)$$

$$\ddot{\theta} = [m_p l^2 (m_p \sin^2 \theta + m_c)]^{-1} \times [(m_p l F_x - d_v m_p l \dot{x}) \cos \theta - d_\omega (m_c + m_p) \dot{\theta} + (-m_p^2 l^2 \dot{\theta}^2 \cos \theta + g m_p^2 l + g m_c m_p l) \sin \theta] \quad (110b)$$

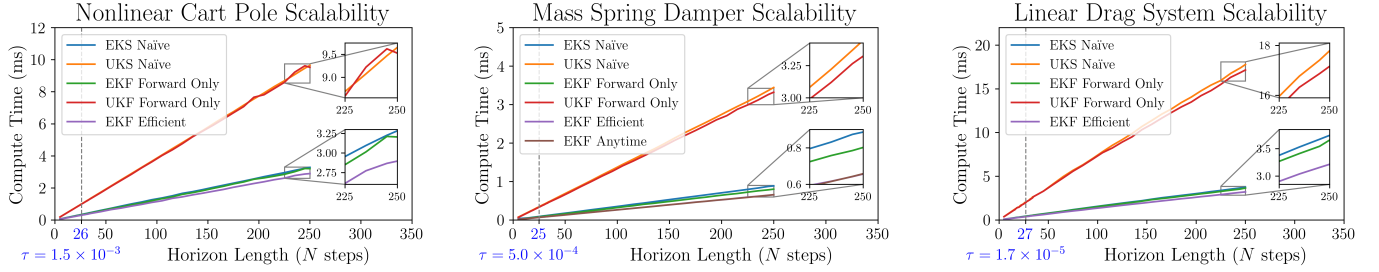


Fig. 8: Computational scalability of every presented algorithm and system as a function of the horizon length N using SQP-like measurement mode for the linear drag system. Notably, observed control scales linearly with N , while most MPC methods scale quadratically. Vertical dashed lines indicate the step count and τ tolerance at which the closed-loop trajectory cost is within 1% of the $N = 1000$ result.

where the parameters are: cart mass $m_c = 0.25\text{kg}$, pole mass $m_p = 0.2\text{kg}$, pole length $l = 0.45\text{m}$, linear damping $d_v = 0.05\text{Ns/m}$, and angular damping $d_\omega = 0.015\text{Nms/rad}$. The objective function used is quadratic and is given by

$$J_{cp} = \sum_{k=0}^N \|\chi - \chi_{ref}\|_{W_{cp}}^2 \chi + (\Delta F_x)^2 W_f \quad (111)$$

where $\chi_{ref} = \vec{0}_\eta$, the weight $W_{cp} = \text{diag}([1000, 1, 300, 25])$ penalizes the state (109) and the weight $W_f = 20$ penalizes changes in control effort. The gradient-based measurement mode was used for both the EKF and UKF versions of Algorithm 2, which is equivalent to the SQP-based measurement mode due to the quadratic nature of (111).

Figure 7 shows the cart pole swing up task performed by observed control with both the EKF and UKF backends, whose results are effectively indistinguishable. This result is consistent with the general understanding that for moderately nonlinear systems such as the cart pole, both EKF and UKF provide reasonably accurate covariance propagation, and thus in observed control, result in equivalent nonlinear controls.

E. Computational Scalability

Control update compute times were benchmarked for each valid algorithm-filter combination and all the presented systems, as shown in Table II. All benchmarks were performed on a single thread of one performance core of an Intel i7-12700K CPU, running Linux (Kubuntu 24.04). The observed control implementation is written in C++20 using Eigen 3.4.0 for matrices, compiled with GCC 13.3 (“-O3 -march=native”). Observed control is implemented as part of a highly flexible and dynamically reconfigurable code base; producing a fixed-memory, problem-specific C/C++ implementation of observed control would yield a

Figure 8 reports the average control update compute times for the cart pole, mass spring damper, and linear drag system examples for a variety of time horizon lengths. The benchmarks validate the expected linear scalability of observed control with respect to N , and demonstrate the efficiency of the estimation-dual formulations. All plots are shown up to $N = 250$, though this greatly exceeds the horizon length necessary for control convergence. Vertical dashed lines in each plot indicate the smallest N and associated τ values at which the total trajectory cost converges to $\leq 1\%$ of the $N = 1000$ result, confirming that additional look-ahead beyond this point

	Naïve		Forward Only		Efficient		Anytime	
	EKS	UKS	EKF	UKF	EKF	UKF	EKF	UKF
Linear	•	•	•	•	•	•	•	•
nonlinear	•	•	•	•	•	•	•	•

TABLE II: Supported combinations of presented observed control algorithms, filtering back-ends, and system linearities.

yields no control improvement and unnecessarily increases compute time. As such, a δ_2 threshold of between 1×10^{-6} and 1×10^{-8} is recommended for τ .

The EKF-backed implementations consistently run faster than their UKF counterparts but show no substantial difference in closed-loop objective performance across the tested nonlinearities. As expected, the efficient implementation is the fastest, followed by the forward-only, and then the naïve (full smoother). Beyond small computational speed improvement, the main benefit of using the efficient formulation is that it contains only one inverse of a small positive-definite matrix at each horizon step, making it more numerically stable on limited-precision (i.e., 32-bit floating point) hardware.

V. CONCLUSION

Observed control leverages the duality between state estimation smoothers and model predictive control to achieve linear time-horizon scalability and adaptive horizons. Any filter that is compatible with RTS smoothers and can support zero process noise can be used as an observed control backend. The presented algorithms (based on Kalman-type filters) inherit their properties—providing optimal controls for linear systems with quadratic penalties and high-quality (near optimal) controls for nonlinear systems or nonquadratic penalties, and demonstrate sub-millisecond single-threaded compute times. Thus, observed control is an attractive, almost plug-and-play MPC algorithm that enables dual-use of existing state-estimation codes for MPC computation that is appropriate for high-rate, resource-constrained, nonlinear predictive control.

VI. REFERENCES

- [1] C. R. Cutler and B. L. Ramaker. Dynamic matrix control – a computer control algorithm. *Joint Automatic Control Conference*, 17:72, 1980.
- [2] J. Richalet, A. Rault, J.L. Testud, and J. Papon. Model predictive heuristic control: Applications to industrial processes. *Automatica*, 14(5):413–428, 1978.

- [3] Max Schwenzer, Muzaffer Ay, Thomas Bergs, and Dirk Abel. Review on model predictive control: an engineering perspective. *The International Journal of Advanced Manufacturing Technology*, 117(5):1327–1349, Nov 2021.
- [4] Moritz Diehl, Hans Joachim Ferreau, and Niels Haverbeke. *Efficient Numerical Methods for Nonlinear MPC and Moving Horizon Estimation*, pages 391–417. Springer Berlin Heidelberg, Berlin, Heidelberg, 2009.
- [5] James B. Rawlings, David Q. Mayne, and Moritz M. Diehl. *Model Predictive Control: Theory, Computation, and Design*. Nob Hill Publishing, 2017.
- [6] Mario Zanon, Andrea Boccia, Vryan Gil S. Palma, Sonja Parenti, and Ilaria Xausa. Direct optimal control and model predictive control. *Optimal control: novel directions and applications*, pages 263–382, 2017.
- [7] Wei C. Li and Lorenz T. Biegler. A multistep, newton-type control strategy for constrained, nonlinear processes. In *1989 American Control Conference*, pages 1526–1527, 1989.
- [8] Toshiyuki Ohtsuka. A continuation/gmres method for fast computation of nonlinear receding horizon control. *Automatica*, 40(4):563–574, 2004.
- [9] Moritz Diehl. Real-time optimization for large scale nonlinear processes. 920, 01 2001.
- [10] Moritz Diehl, Hans Bock, and Johannes Schlöder. A real-time iteration scheme for nonlinear optimization in optimal feedback control. *SIAM J. Control and Optimization*, 43:1714–1736, 01 2005.
- [11] Victor M. Zavala and Lorenz T. Biegler. The advanced-step nmhc controller: Optimality, stability and robustness. *Automatica*, 45(1):86–93, 2009.
- [12] Boris Houska, Hans Joachim Ferreau, and Moritz Diehl. An auto-generated real-time iteration algorithm for nonlinear mpc in the microsecond range. *Automatica*, 47(10):2279–2285, 2011.
- [13] B. Houska, H.J. Ferreau, and M. Diehl. ACADO Toolkit – An Open Source Framework for Automatic Control and Dynamic Optimization. *Optimal Control Applications and Methods*, 32(3):298–312, 2011.
- [14] David Ariens, Moritz Diehl, Hans Joachim Ferreau, Boris Houska, Filip Logist, Rien Quirynen, and Milan Vukov. *ACADO Toolkit User's Manual*, 2014. Available at: <https://acado.github.io/documentation.html>.
- [15] Robin Verschueren, Gianluca Frison, Dimitris Kouzoupis, Niels van Duijkeren, Andrea Zanelli, Rien Quirynen, and Moritz Diehl. Towards a modular software package for embedded optimization. *IFAC-PapersOnLine*, 51(20):374–380, 2018. 6th IFAC Conference on Nonlinear Model Predictive Control NMPC 2018.
- [16] Jorge Nocedal and Stephen J. Wright. *Numerical Optimization*. Springer New York, NY, 2006.
- [17] Gianluca Frison and Moritz Diehl. Hpipm: a high-performance quadratic programming framework for model predictive control. *IFAC-PapersOnLine*, 53(2):6563–6569, 2020. 21st IFAC World Congress.
- [18] Sebastien Gros, Mario Zanon, Rien Quirynen, Alberto Bemporad, and Moritz Diehl. From linear to nonlinear mpc: bridging the gap via the real-time iteration. *International Journal of Control*, 93:1–19, 09 2016.
- [19] Grady Williams, Paul Drews, Brian Goldfain, James M. Rehg, and Evangelos A. Theodorou. Aggressive driving with model predictive path integral control. In *2016 IEEE International Conference on Robotics and Automation (ICRA)*, pages 1433–1440, 2016.
- [20] Grady Williams, Brian Goldfain, Paul Drews, Kamil Saigol, James Rehg, and Evangelos Theodorou. Robust sampling based model predictive control with sparse objective information. 06 2018.
- [21] Manan S. Gandhi, Bogdan Vlahov, Jason Gibson, Grady Williams, and Evangelos A. Theodorou. Robust model predictive path integral control: Analysis and performance guarantees. *IEEE Robotics and Automation Letters*, 6(2):1423–1430, 2021.
- [22] Ziyi Wang, Oswin So, Jason Gibson, Bogdan Vlahov, Manan Gandhi, Guan-Hong Liu, and Evangelos Theodorou. Variational inference mpc using tsallis divergence. 07 2021.
- [23] Isin Balci, Efsthios Bakolas, Bogdan Vlahov, and Evangelos Theodorou. Constrained covariance steering based tube-mppi. pages 4197–4202, 06 2022.
- [24] Ji Yin, Zhiyuan Zhang, Evangelos Theodorou, and Panagiotis Tsiotras. Trajectory distribution control for model predictive path integral control using covariance steering. In *2022 International Conference on Robotics and Automation (ICRA)*, pages 1478–1484, 2022.
- [25] Hilbert J. Kappen. Linear theory for control of nonlinear stochastic systems. *Phys. Rev. Lett.*, 95:200201, Nov 2005.
- [26] Lars Grune and Anders Rantzer. On the infinite horizon performance of receding horizon controllers. *IEEE Transactions on Automatic Control*, 53(9):2100–2111, 2008.
- [27] S. S. Keerthi and E. G. Gilbert. Optimal infinite-horizon feedback laws for a general class of constrained discrete-time systems: Stability and moving-horizon approximations. *Journal of Optimization Theory and Applications*, 57(2):265–293, May 1988.
- [28] Bei Hu and A. Linnemann. Toward infinite-horizon optimality in nonlinear model predictive control. *IEEE Transactions on Automatic Control*, 47(4):679–682, 2002.
- [29] G. Grimm, M.J. Messina, S.E. Tuna, and A.R. Teel. Model predictive control: for want of a local control lyapunov function, all is not lost. *IEEE Transactions on Automatic Control*, 50(5):546–558, 2005.
- [30] James A. Primbs and Vesna Nevistić. Feasibility and stability of constrained finite receding horizon control. *Automatica*, 36(7):965–971, 2000.
- [31] A. Jadbabaie and J. Hauser. On the stability of receding horizon control with a general terminal cost. *IEEE Transactions on Automatic Control*, 50(5):674–678, 2005.
- [32] Andrea Boccia, Lars Grüne, and Karl Worthmann. Stability and feasibility of state constrained mpc without stabilizing terminal constraints. *Systems & Control Letters*, 72:14–21, 2014.
- [33] J.S. Shamma and Dapeng Xiong. Linear nonquadratic optimal control. *IEEE Transactions on Automatic Control*, 42(6):875–879, 1997.
- [34] R. E. Kalman. A New Approach to Linear Filtering and Prediction Problems. *Journal of Basic Engineering*, 82(1):35–45, 03 1960.
- [35] R. E. Kalman and R. S. Bucy. New results in linear filtering and prediction theory. *Journal of Basic Engineering*, 83(1):95–108, 03 1961.
- [36] Emanuel Todorov. General duality between optimal control and estimation. In *2008 47th IEEE Conference on Decision and Control*, pages 4286–4292, 2008.
- [37] Jin W. Kim and Prashant G. Mehta. Duality for nonlinear filtering I: Observability. *IEEE Transactions on Automatic Control*, 69(2):699–711, 2024.
- [38] Jin Won Kim and Prashant G. Mehta. Duality for nonlinear filtering II: Optimal control. *IEEE Transactions on Automatic Control*, 69(2):712–725, 2024.
- [39] Sanjoy K. Mitter and Nigel J. Newton. A variational approach to nonlinear estimation. *SIAM Journal on Control and Optimization*, 42(5):1813–1833, 2003.
- [40] H. E. Rauch, F. Tung, and C. T. Striebel. Maximum likelihood estimates of linear dynamic systems. *AIAA Journal*, 3(8):1445–1450, 1965.
- [41] Mohinder S. Grewal and Angus P. Andrews. *Kalman Filtering: Theory and Practice Using MATLAB®*. Wiley, 4th edition, 2015.
- [42] Simon J. Julier and Jeffrey K. Uhlmann. New extension of the kalman filter to nonlinear systems. In *Signal processing, sensor fusion, and target recognition VI*, volume 3068, pages 182–193. SPIE, 1997.
- [43] Richard L. Pratt, Brooke E. Suesser, and Andrew J. Petruska. Observed control of magnetic continuum devices. *Robotics*, 12(1), 2023.
- [44] Vassilis L. Syrmos Frank L. Lewis, Draguna L. Vrabie. *Optimal Control*. John Wiley & Sons, Ltd, 2012.
- [45] Francesco Borrelli, Alberto Bemporad, and Manfred Morari. *Predictive Control for Linear and Hybrid Systems*. Cambridge University Press, 2017.
- [46] Bradley M. Bell. The iterated kalman smoother as a gauss-newton method. *SIAM Journal on Optimization*, 4(3):626–11, 08 1994. Copyright - Copyright] © 1994 Society for Industrial and Applied Mathematics; Last updated - 2023-12-04.
- [47] R. E. Kalman. Contributions to the theory of optimal control. *Boletín de la Sociedad Matemática Mexicana*, 5:102–119, 1960.
- [48] Dan Simon. *Optimal State Estimation: Kalman, H-infinity, and Nonlinear Approaches*. Wiley-Interscience, 1st edition, 2006.